



Dynamic Transport and Distribution of Organic Pollutants in Water and Sediments of the Rur River

Christina A. Schwanen · Pia M. Kronsbein ·
Berna Balik · Jan Schwarzbauer 

Received: 9 August 2023 / Accepted: 27 November 2023 / Published online: 19 December 2023
© The Author(s) 2023

Abstract The distribution and fate of organic pollutants within different compartments of a river system are determined by several key effects and drivers. Within the scope of this study, the aqueous and sedimentary compartments have been analyzed complementary to understand transport and accumulation pathways and to determine temporospatial effects. The bi-annual campaigns allow general statements to be made about relevant processes and effects on pollutant distribution. GC/MS non-target screenings revealed that there is only a minor group of contaminants that occur both in the water and in the riverbed. Nevertheless, for both phases, the main contamination with organic compounds occurred in the anthropogenic, middle to lower course of the river with loads up to 18.3 kg/d (2,4,7,9-tetramethyl-5-decyne-4,7-diol, TMDD) in the water and amounts up to 3.3 mg/g_{TOC} (ΣEPA16 polycyclic aromatic hydrocarbons, PAHs) in the riverbed. Main emission sources were comparable, resulting in a high, almost constant contamination level which also contributes to the pollution of the superior, receiving river. Indeed, the pollution transport of the aqueous and sedimentary phases was closely connected, but with slight temporal and spatial heterogeneities. For the aqueous

compartment, seasonal effects were identified while a remarkable change in riverbed contamination occurred due to an extreme flood event. However, dams within the catchment system cause a disconnection of the transport of lipophilic and hydrophilic substances. Overall, the combined investigation of different phases is an important aspect for a comprehensive view of river and environmental contamination.

Keywords Organic pollution · River compartments · Fluvial transport · Emission patterns

1 Introduction

Despite the increase in environmental awareness, rivers remain important for various anthropogenic activities and are intensively used, e.g., for shipping, water withdrawal, and discharge of treated wastewater. Accordingly, river systems worldwide have been and continue to be strongly affected by the introduction of a heterogeneous mixture of anthropogenic contaminants (Lin et al., 2017). Overall, rivers can therefore be defined as transitional systems for pollutants between their source and deposition areas (Esser et al., 2020).

In particular, low-molecular-weight organic contaminants such as pesticides or pharmaceuticals are of high environmental relevance as they are often toxic and bioaccumulative and can persist for long periods in environmental compartments (Bernhardt

C. A. Schwanen · P. M. Kronsbein · B. Balik ·
J. Schwarzbauer (✉)
Institute of Organic Biogeochemistry in Geo-Systems,
RWTH Aachen University, Lochnerstraße 4-20,
52056 Aachen, Germany
e-mail: jan.schwarzbauer@emr.rwth-aachen.de

et al., 2017; Morin-Crini et al., 2021; Wilkinson et al., 2017). These substances are very diverse and show a large structural variety as they are also used in a wide range of applications (Petrovic et al., 2016; Schwarzenbach et al., 2010). In combination with specific environmental conditions, this diversity results in numerous dispersal mechanisms, pathways, different distribution ranges, and accumulation sites.

For instance, hydrophilic components accumulate primarily in the aqueous phase and can therefore be rapidly transported within river systems (Heim et al., 2004). Due to their different chemical and physical behavior, these compounds show a high environmental mobility. In combination with the high dynamics of the watery river compartment, transport and distribution processes are usually very short-term, but still complex and challenging to analyze. In contrast, hydrophobic respectively lipophilic contaminants tend to be enriched in sedimentary material. In a river system, this includes suspended particulate matter as well as river sediment, but also material on floodplains or in reservoirs. Due to the more anaerobic conditions, sediments often act as a sink for lipophilic organic pollutants (Dsikowitzky et al., 2020; Heim et al., 2004). However, this is not limited to floodplains, as pollutants also accumulate in the hyporheic zone at the riverbed (Gandy et al., 2007; Lawrence et al., 2013; Weatherill et al., 2018). Although the particulate compartment is clearly less dynamic than the aqueous phase, different transport and (re)mobilization pathways of pollutants need to be considered for holistic risk and hazard assessments. Especially riverbed sediments can be easily mobilized due to changes in flow dynamics and annual discharge patterns (Cofalla et al., 2012; Westrich & Förstner, 2007).

Therefore, for a comprehensive assessment of the dynamic and long-term impact potential of organic substances in a complex river system, it is crucial to consider both the particulate and the aqueous phases in a complementary manner (e.g., Ferreira da Silva et al., 2011). However, most studies focus on a single compartment or on a single sampling campaign. Nevertheless, only regular sampling and monitoring of several compartments can provide reliable, general statements on relevant processes and effects on the pollutant distribution and accumulation. In addition, the consideration of different substances is also crucial and should cover the high diversity in terms

of molecular structures as well as physicochemical properties (e.g., lipophilic vs. hydrophilic; polar vs. non-polar).

This is the first study to consider regular sampling of different compartments with a high spatial coverage on the Rur river. The Rur itself is a typical meso-scaled river in Central Europe, which originates in the High Fens in Belgium, covers most of its flow distance in Germany, and finally discharges into the Meuse at Roermond (Netherlands). It has a total length of 163 km and a catchment area of about 2340 km² (Staatliches Umweltamt Aachen, 2005). Generally, it is divided into two physiographic parts: a typical low mountain range landscape of the Eifel in the South and the northern lowland part belonging to the Lower Rhine Embayment. Along its river course, it shows a complex picture of anthropogenic impacts such as river regulation, water withdrawal, and discharge of treated wastewater. However, most of the world's river systems are anthropogenically influenced (Best, 2019; Ekka et al., 2020; Notebaert et al., 2018; Tockner et al., 2009). Therefore, the Rur river system is well suited for the analysis of input, transport, and deposition of various pollutants due to the diverse but clearly definable influences and emission sources. Processes and effects can be correlated with specific conditions and thus enable transferability to other river systems.

The main objectives were to determine the contaminant inventories in the different compartments and to understand distinct transport and accumulation pathways and processes. Differences in the contamination situation of the specific compartments and the general distribution of pollutants were identified. In particular, spatial, seasonal, and temporal variations in the state of pollution were investigated. Therefore, pollutant loads, amounts, and mass fluxes were determined, and emission profiles were established for a distinct emission characteristic and for a holistic assessment of environmental fate and behavior.

2 Methods

2.1 Study Area and Sampling

As mentioned above and shown in Fig. 1, the Rur catchment consists of two different physiographic zones, which are relevant for different pollutant

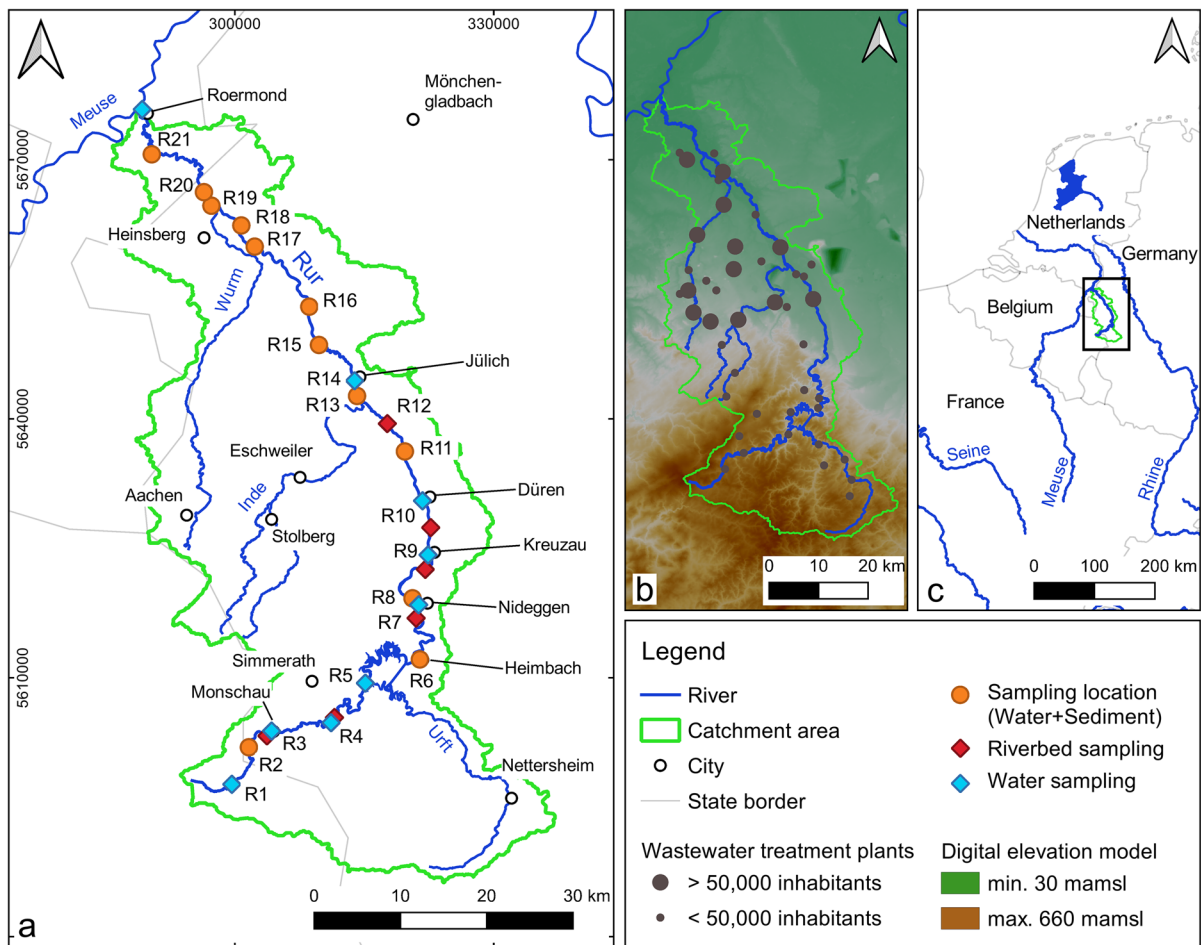


Fig. 1 **a** Overview of the Rur catchment (North Rhine-Westphalia, Germany) including sampling locations and tributaries. **b** Shows wastewater treatment plants and elevation. **c** Shows

the catchment in a European context; coordinate system: ETRS89/UTM zone 32N

emissions and distributions. In the southern upper course, the flow dynamics are mostly close to a natural state. However, various dams and reservoirs determine the flow pattern, which are among others of great importance for drinking water supply and flood protection (Wasserverband Eifel-Rur, 2017a). They also play an important role in sediment and suspended matter retention (Wolf et al., 2022). The middle and lower courses of the Rur are more anthropogenically influenced by various industries (e.g., paper, metal, and textile processing), lignite mining, and agriculture (Staatliches Umweltamt Aachen, 2005). In addition, several wastewater treatment plants (WWTPs) discharge their effluents into the Rur and its tributaries (especially Inde and Wurm). Overall, more than

40 WWTPs are located in the catchment area, with the WWTP Aachen-Soers (on the tributary Wurm) and the WWTP Düren-Merken being the largest and most relevant dischargers (Wasserverband Eifel-Rur, 2017c).

The samples were taken at two different seasons according to the annual flow pattern of the Rur river. Sampling was carried out along the entire course of the river to account for differences in the landscape, hydrological conditions and anthropogenic influences. A total of four sampling campaigns was performed between November 2020 and May 2022 (cf. Table 1). Grab water samples (1 L) were scooped from midstream of the river close to the water surface. Sediment samples (200 to 300 g) were collected

Table 1 Overview of the sampling campaigns and the number of samples taken from different compartments (river water and riverbed)

Sampling campaign	Date	Number of samples	
		Water	Sediment
1	November 23–24, 2020	21	17
2	June 15–16, 2021	20	17
3	November 23–24, 2021	21	18
4	May 11–12, 2022	21	18

from the same river sections in stillwater zones near to the riverbanks. At some sites (e.g., in Monschau (R3) and Roermond (R22)), collection of sediment samples was not possible in the immediate vicinity of the water sample location and needed to be moved. Thus, water and sediment sampling locations differ slightly from each other in some cases (cf. Tables 2 and 3).

All samples (sediment and water) were stored in solvent-cleaned glass flasks in the dark at 4 °C prior to extraction. The sampling, extraction, and

measurement procedures were the same for all sampling campaigns.

2.2 Total Organic Carbon Analysis

For sediment samples, the content of total organic carbon (TOC), total carbon (TC), and total inorganic carbon (TIC) was determined. 100 mg dried sample aliquots were heated and ashed in a furnace (liqui-TOC II; Elementar Analysensysteme GmbH, Langenselbold, Germany) at 550 °C (TOC) and 1000 °C (TIC). Subsequently, TOC concentrations were used for normalization of the sediment samples to ensure comparability between samples and different campaigns.

2.3 Organic Geochemical Analysis

2.3.1 Water Sample Extraction and Fractionation

Sample treatment and analysis followed well-established and previously described methods (Dsikowitzky et al., 2002; Schwanen & Schwarzbauer, 2022).

Table 2 Overview of the water samples and the corresponding river runoff data from several gages along the Rur river in November 2020, June 2021, November 2021, and May 2022

Site no.	River km	Gage	River runoff MQ [m ³ /s]			
			Nov. 2020	Jun. 2021	Nov. 2021	May 2022
R1	159.5	Monschau	1.7	0.5	0.8	1.1
R2	152.8	Monschau	1.7	0.5	0.8	1.1
R3-W	148.1	Monschau	1.7	0.5	0.8	1.1
R4-W	137.9	Dedenborn	2.2	1.1	1.9	1.1
R5	124.5	Dedenborn/Heimbach	3.0	5.0	4.0	2.7
R6	109.3	Heimbach	5.0	9.1	7.4	4.4
R7-W	96.6	Zerkall	6.2	9.1	7.6	4.7
R8	94.2	Zerkall	6.2	9.1	7.6	4.7
R9-W	84.2	Obermaubach	5.0	9.9	7.9	5.0
R10-W	77.3	Obermaubach	5.0	9.9	7.9	5.0
R11	71.0	Obermaubach/Jülich	7.0	11.5	7.7	5.3
R13	61.4	Jülich	9.4	12.8	7.5	5.6
R14	59.6	Jülich	9.4	12.8	7.5	5.6
R15	51.2	Jülich/Linnich	9.0	12.0	9.0	7.0
R16	46.2	Jülich/Linnich	9.0	12.0	9.0	7.0
R17	34.7	Jülich/Linnich	9.0	12.0	9.0	7.0
R18	30.8	Jülich/Linnich	9.0	12.0	9.0	7.0
R19	26.2	Stah	8.8	11.2	11.4	8.5
R20	24.2	Stah	8.8	11.2	11.4	8.5
R21	10.4	Stah	8.8	11.2	11.4	8.5
R22	0.3	Stah	8.8	11.2	11.4	8.5

Table 3 Overview of the sediment samples and the corresponding TOC content in November 2020, June 2021, November 2021, and May 2022

Site no.	River km	TOC [%]			
		Nov. 2020	Jun. 2021	Nov. 2021	May 2022
R2	152.8	n.s.	1.27	0.64	0.91
R3-S	148.9	0.49	0.74	0.70	1.00
R4-S	136.1	0.67	0.68	0.45	0.83
R6	109.3	0.92	0.63	1.08	0.73
R7-S	98.6	1.22	1.15	0.46	0.44
R8	94.2	0.17	5.69	0.50	4.31
R9-S	86.3	0.67	0.55	0.52	0.60
R10-S	80.7	0.34	0.28	0.66	0.35
R11	71.0	0.17	0.28	0.53	0.31
R12	66.9	1.18	3.73	0.89	2.67
R13	61.4	0.24	1.85	0.22	0.31
R14	59.6	0.58	0.52	0.68	0.49
R15	51.2	1.57	5.31	1.72	1.27
R16	46.2	1.00	1.29	0.34	0.78
R17	34.7	0.35	0.73	0.71	2.36
R18	30.8	0.23	0.90	0.55	1.34
R19	26.2	0.27	n.s.	0.52	2.11
R20	24.2	1.13	4.50	1.84	3.89

n.s., not sampled

First, water samples were filtered through pre-cleaned GF/F filters (Macherey–Nagel, Düren, Germany) to remove suspended particulate matter. Then, a sequential liquid–liquid extraction was performed by adding 50 mL each of *n*-pentane (fraction 1) and dichloromethane (fraction 2) to the 1-L-aliquots.

Both fractions were spiked with 50 µL of an internal standard solution consisting of the reference compounds benzophenone-*d*₁₀ (6.3 ng/µL), hexadecane-*d*₃₄ (6.0 ng/µL), and fluoroacetophenone (5.8 ng/µL). In the following, the extracts were concentrated to volumes of approximately 2 mL and dried with anhydrous granulated sodium sulfate (Na₂SO₄). Prior to injection, fractions 1 and 2 were concentrated to final volumes of 10 to 100 µL.

2.3.2 Sediment Sample Extraction and Fractionation

According to Schwanen et al. (2023), aliquots of 15 to 20 g of untreated sediment were extracted using accelerated solvent extraction (ASE).

Approximately 30 mL of acetone, acetone/*n*-hexane (1: 1; v: v), and *n*-hexane were used for sequential extraction. The extraction cell was kept at a pressure of 10 MPa and a temperature of 100 °C for 5 min each. In the following, the extracts were combined and dried with anhydrous granulated sodium sulfate (Na₂SO₄). Finally, they were desulphurized by the addition of activated copper in combination with ultrasonic treatment and concentrated to a volume of 0.5 mL.

For fractionation, mixtures of *n*-pentane, dichloromethane, and methanol were used according to the polarity of the organic contaminants. In the end, 6 fractions were obtained (B1 5 mL *n*-pentane; B2 8.5 mL *n*-pentane/DCM 95/5; B3 5 mL *n*-pentane/DCM 90/10; B4 5 mL *n*-pentane/DCM 40/60; B5 5 mL DCM; B6 5 mL methanol). The acidic compounds in fraction B6 required further methylation by addition of BF₃-methanol (B6K1 3 mL *n*-pentane/DCM 40/60 plus 6 mL DCM; B6K2 5 mL methanol). 50 µL of the above-mentioned internal standard was added to fractions B1 to B5 and 200 µL to fraction B6K1. Prior to GC/MS analyses, all fractions were reduced to final volumes of 20 to 400 µL (B1 to B5) respectively 100 to 800 µL (B6).

2.3.3 Gas Chromatography–Mass Spectrometry Analyses

Gas chromatographic/mass spectrometric (GC/MS) analyses were performed on a quadrupole ThermoQuest Trace MS mass spectrometer coupled with a ThermoQuest Trace GC which was equipped with a ZB-5 fused silica capillary column (Phenomenex, Aschaffenburg, Germany; 30 m×0.25 mm ID×0.25 µm film thickness). The flow of the carrier gas helium was set to 1.5 mL/min. For all fractions (water and sediment), the temperature program and gas chromatographic conditions were a 1 µL injection (injector temperature of 270 °C) at 60 °C with a splitless time of 60 s, 3 min at the initial temperature, and then programmed to 310 °C at a rate of 3 °C/min followed by 20 min isothermal time. The mass spectrometric operation took place in full-scan mode (EI⁺, 70 eV) with a source temperature of 200 °C, scanning from 35 to 700 amu at a rate of 1.5 scans/s.

2.3.4 Compound Identification and Quantification

Identification of organic compounds was based on a comparison with mass spectral databases (e.g., NIST) and previously published information. Further on, they were verified by comparing specific gas chromatographic and mass spectral parameters (e.g., retention times and elution orders) with those of purchased reference materials. Quantitative data were obtained by peak integration of characteristic ion chromatograms and determined using external four-point calibrations. Compound concentrations were within the range of expected values in the samples and within the linear detection range. To correct injection and sample volume inaccuracies, a surrogate standard was used. The quantification limits were in the range of 5 ng/g_{TOC} in sediment samples and 5 ng/L in water samples (calculation based on signal-to-noise ratios in real sample matrices). Furthermore, blank analyses were performed to determine possible background contamination ($n=4$ for both water and sediment samples). They revealed negligible concentrations of several plasticizers such as phthalates and triacetin and tocopheryl acetate, some PAHs, DIPNs, and BHT. Detailed information on recovery rates can be found in previous studies (Schwanen & Schwarzbauer, 2022; Schwanen et al., 2023).

3 Results and Discussion

Emission profiles were established for substances in both the aqueous and the sedimentary phase over the entire course of the river. As different river run-offs (cf. Table 2) can strongly affect the compound concentrations in river water, loads, L (g/d), were calculated using the specific concentration in water, C (ng/L), and the median river runoff, MQ (m³/s): $L = C \times MQ \times (3600 \times 24 / 10^6)$ (Dsikowitzky et al., 2004).

The amounts of the sediment samples were also normalized to allow better comparability between different locations as well as campaigns. In particular, the TOC content has a major influence on the pollutant distribution and accumulation; hence, a TOC normalization was performed. As shown in Table 3, the TOC content was between 0.2 and 5.7%. The TOC concentrations and the variability along the river course were very low in the winter sampling

campaigns (Nov. 2020: 0.2 to 1.6%; Nov. 2021: 0.2 to 1.8%). Both were higher and more pronounced in June 2021 and May 2022 (Jun. 2021: 0.3 to 5.7%; May 2022: 0.3 to 4.3%). Similar seasonal distributions were observed in the Odra river (Poland). They are probably related to increased biological activities and subsequently higher primary production in summer (Kubo & Kanda, 2017; Niemirydz et al., 2006).

The loads, amounts, and emission profiles were used to identify triggers and drivers of environmental behavior. Additional information on the toxicity of various substances identified in the Rur catchment area can be found in the Supplementary Material. Based on the data measured for the Rur river, some basic implications can be deduced about pollutant behavior and associated processes in the environment. However, there is only a small group of contaminants in this river system that occur in both the aqueous and particulate phases. Therefore, it is reasonable to consider these phases separately to derive environmental fate and transport.

3.1 River Water

The aqueous phase is a highly dynamic compartment with a generally fast and continuous pollutant transport, so that any sampling campaign is only a snapshot of the respective contamination. Nevertheless, emission profiles can be used to identify general trends and to determine specific fates and behaviors, as the framework conditions have not changed over the period considered (e.g., WWTP features, population development, and water demand).

Previous non-target screening from sampling campaign 1 (Nov. 2020) revealed a high structural diversity of various lipophilic to semi-polar substances within the aqueous phase of the Rur river (Schwanen & Schwarzbauer, 2022). Indeed, a high level of structural diversity (~60 compounds) was found in all sampling campaigns during the observation period. In general, these substances can be assigned to different categories based on their (technical) application or chemical structures. Among others, pharmaceuticals, biocides, and constituents of personal care products and several industrial compounds have been identified. Contamination levels were generally similar across all sampling campaigns. An overview of the determined loads is given in Table 4. The main contamination occurred in the middle to lower reaches of

the Rur river. This roughly reflects the anthropogenic influence on the catchment system, as this region is heavily populated and used for industrial and agricultural purposes. For comparison with other studies, it is usually necessary to use concentrations, as many authors do not specify any loads. However, it should be noted that for river systems, loads are clearly more informative, as they are independent of the specific runoff and thus allow comparability of different discharge situations and hence different river systems.

Overall, the highest loads were detected for the industrial substance 2,4,7,9-tetramethyl-5-decyne-4,7-diol (TMDD), which is probably related to its use in the paper industry in the Rur catchment (up to 18.3 kg/d). In general, considerable pollution occurred downstream of the WWTP Düren (R11), which also treats wastewater from paper production. Only slightly higher concentrations were found in the effluents of German and Swedish WWTPs (maxima: ~18.3 µg/L (Rur river, this study), 37 µg/L (Swedish WWTP effluent), and 28 µg/L (German WWTP effluent)) indicating the high contamination of the Rur river itself (Dsikowitzky et al., 2015; Sternbeck et al., 2012).

Further on, methyl dehydroabietate and triacetin were found with loads in the range of kilograms per day. Methyl dehydroabietate (up to 11.9 kg/d) is widely used in cosmetic formulations as an emollient and skin care agent. It is therefore likely to be introduced via wastewater effluents (Bährle-Rapp, 2007). However, it is also known to be a toxic anti-estrogenic organic agent used in the paper industry, and the maximum value found was similar to the effluent concentration from a Canadian paper mill (Terasaki et al., 2009; Wartman et al., 2009). The plasticizer triacetin (up to 6.6 kg/d) also has several industrial applications (e.g., in the paper industry). In general, the occurrence of both substances was rather diffuse and could not be clearly assigned to any emission source.

Another substance probably originating from paper production is the industrial substance 1,2-diphenoxyethane (DPE). Between November 2020 and November 2021, the respective maximum loads (between 6 and 20 g/d) occurred behind the inflow of the tributary Kall (R8). This is possibly caused by a paper factory located in Zerkall near the confluence of Kall and Rur. Yet, the paper factory was severely damaged by an extreme summer flood in July 2021, which led to a temporary closure (Aachener Zeitung,

2021). In addition, load increases in the industrial centers of Düren and Jülich (R10 and R14) were observed in the emission profile of November 2021. Paper factories are again a possible source of emissions at these locations. In May 2022, the highest loads (94 g/d) also occurred in the industrially characterized lower course of the Rur river. The distribution was similar in Indonesian surface waters, where DPE was mainly found in industrial and urban areas (Dsikowitzky et al., 2017). However, concentrations of up to 3.3 µg/L were clearly higher than the maximum concentration at the Rur (128 ng/L).

Overall, the paper industry has a major influence on the contamination of the Rur river. In particular, online trade and the associated delivery services have increased the demand for packaging. As a result, paper producers along the Rur have also greatly expanded their production capacities (Kaleß et al., 2020). This may have led to higher levels of contamination with specific compounds.

Besides the high impact of the paper industry, compounds emitted from other applications have also been detected. Due to its antioxidant properties and use in anti-aging cosmetics, tocopheryl acetate is likely to be introduced by municipal wastewater effluents (Silva et al., 2019). Its occurrence in the Rur river was in the load range of kg/d (maximum of 1.4 kg/d in May 2022), but rather diffuse in all sampling campaigns. Eganhouse and Kaplan (1985) investigated tocopheryl acetate as a possible marker for municipal waste in the environment and detected concentrations of 6 to 25 µg/L in the effluents of various WWTPs in California (USA). The maximum concentration found in the Rur river was 3.1 µg/L, while the average concentrations of the four sampling campaigns were in the range of 31 to 475 ng/L.

The antiepileptic drug carbamazepine was regularly identified throughout the Rur, with loads of up to 124 g/d. It showed a downstream increasing contamination correlating well with the adjacent land use, the population density and, thus, the contributions from WWTPs. In fact, besides the WWTP in Düren (discharging directly into the Rur river; R11), the ones in Jülich (discharging directly into the Rur river; between R14 and R15) and in Aachen (discharging into the Wurm tributary; R19) were the main emitters within this river system (Schwanen & Schwarzbauer, 2022). The increasing trend is related to carbamazepine's high stability in the environment, but also

Table 4 Span of minimum and maximum loads [g/d] of organic compounds detected in Rur river water samples (taken in November 2020, June 2021, November 2021, and May 2022)

No.	Compounds	Detected loads [g/d]			
		Nov. 2020	Jun. 2021	Nov. 2021	May 2022
Pharmaceuticals					
1	Carbamazepine	n.d.–124	n.d.–55	n.d.–107	n.d.–115
2	Oxcarbazepine	n.d.–17	n.d.–<6	n.d.–<5	n.d.
3	Caffeine	n.d.–110	n.d.–133	n.d.–142	n.d.–133
4	Lidocaine	n.d.–125	n.d.–96	n.d.–233	n.d.–74
Personal care products					
5	Tocopheryl acetate	n.d.–48	n.d.–523	n.d.–1019	n.d.–1355
6	N,N,N',N'-Tetraacetylenediamine, TAED	n.d.–59	n.d.–39	n.d.–37	n.d.–8
7	4-Methoxycinnamic acid 2-ethylhexylester	n.d.–<4	1–22	n.d.–7	n.d.
8	Drometrizole	n.d.–<4	n.d.–<0.2	n.d.–6	n.d.
9	Galaxolide	n.d.–56	<0.2–78	<0.4–223	<0.5–63
10	Tonalide	n.d.–5	<0.2–6	n.d.–9	n.d.–9
11	4-Oxoisophorone	1–12	1–15	<0.4–9	1–9
12	Lilial	n.d.–<4	n.d.–19	n.d.–<5	n.d.
13	Dihydromethyljasmonate	3–29	1–72	1–64	4–153
14	Coumarin	n.d.–19	n.d.–<6	n.d.–7	n.d.–6
15	4-tert-Butylcyclohexanone	n.d.–9	n.d.–<6	n.d.–<5	n.d.
16	Benzophenone	<1–18	0.2–7	<0.4–20	<0.5–30
17	Isopropyl laurate	22–271	7–498	3–346	2–1337
18	Isopropyl palmitate	3–48	18–978	n.d.–157	n.d.–16
19	Methyl dehydroabietate	122–3078	8–5543	19–11,907	47–3860
Pesticides and biocides					
20	N,N-Diethyl- <i>m</i> -toluamide, DEET	n.d.–27	1–45	n.d.–17	n.d.–55
Technical additives, plasticizers, and other industrial compounds					
21	Di- <i>iso</i> -propylnaphthalenes, DIPNs	n.d.–<4	n.d.–<6	n.d.–<5	n.d.–<2
22	N-Butylbenzenesulfonamide, NBBS	n.d.–67	<0.3–32	<0.4–40	n.d.–79
23	2,4,4-Trimethylpentane-1,3-dioldi- <i>iso</i> -butyrate, TXIB	3–42	<0.2–102	<0.4–26	1–101
24	2,4,7,9-Tetramethyl-5-decyne-4,7-diol, TMDD	4–14,294	4–15,408	<1–18,287	1–12,194
25	(1-Hydroxycyclohexyl)phenylketone, Irgacure 184	n.d.–16	n.d.–41	2–292	4–126
26	Triethylcitrate	1–70	n.d.–44	0.5–31	16–730
27	Acetyl tributylcitrate	n.d.–48	n.d.–28	n.d.–19	n.d.–235
28	Triacetin	234–6579	n.d.–6383	n.d.–934	n.d.–6133
29	Triethyl phosphate	n.d.–158	1–174	n.d.–196	n.d.–135
30	Tributyl phosphate	n.d.–13	n.d.–9	n.d.	n.d.–259
31	Tris(2-chloroethyl)phosphate, TCEP	n.d.–8	n.d.–8	n.d.–81	n.d.–18
32	Tris(chloropropyl)phosphate, TCPP	<1–68	0.3–61	n.d.–130	<0.5–72
33	Triphenyl phosphate	n.d.	n.d.–<6	<0.4–<5	n.d.
34	Triphenylphosphine oxide	n.d.–206	n.d.–79	n.d.–140	n.d.–130
35	Dimethyl phthalate	2–52	2–57	<0.4–35	1–17
36	Diethyl phthalate	12–117	8–168	2–189	6–112
37	Di- <i>iso</i> -butyl phthalate	19–370	9–451	10–106	20–599
38	Di- <i>n</i> -butyl phthalate	33–970	24–703	23–298	49–473
39	Benzyl butyl phthalate	n.d.–12	n.d.–56	n.d.–14	<0.5–86
40	Bis(2-ethylhexyl) phthalate, DEHP	105–1060	n.d.–1580	n.d.–675	n.d.–1134

Table 4 (continued)

No.	Compounds	Detected loads [g/d]			
		Nov. 2020	Jun. 2021	Nov. 2021	May 2022
41	2,2-Dimethoxy-1,2-diphenylethanone, DMPA	n.d.–24	n.d.–<6	n.d.–16	n.d.–23
42	Diphenoxyethane, DPE	n.d.–6	<0.2–7	n.d.–20	2–48
	Miscellaneous contaminants				
	Halogenated compounds				
43	Dichloroaniline	n.d.–6	n.d.–15	n.d.–6	n.d.–<2
44	1,1,2,2-Tetrachloroethane	n.d.–253	n.d.–28	n.d.–167	n.d.–108
	S-containing compounds				
45	Diphenyl sulfone	n.d.–14	n.d.–<6	n.d.–9	n.d.–2613
46	Methylphenylsulfone	n.d.–25	n.d.–7	n.d.–20	n.d.–22
47	Benzothiazole	n.d.–6	<0.2–7	n.d.–6	n.d.–<2
48	2-Methylthiobenzothiazole	n.d.–42	<0.2–32	n.d.–48	n.d.–76
49	N-Phenylbenzenesulfonamide	n.d.–25	n.d.–251	n.d.–15	n.d.–114
50	N-Ethyl- <i>o</i> -toluenesulfonamide	n.d.–111	n.d.–32	n.d.–66	n.d.–49
51	N-Ethyl- <i>p</i> -toluenesulfonamide	n.d.–149	n.d.–25	n.d.–57	n.d.–69
	N-containing compounds				
52	2-Methylbenzotriazole	n.d.–217	n.d.–70	n.d.–84	n.d.–27
53	Quinoline	n.d.–15	n.d.–6	n.d.–<5	n.d.–<2
54	2,3-Diethyl-2,3-dimethylsuccinonitrile	n.d.–<4	n.d.	n.d.	n.d.
55	Phenylisocyanate	n.d.–129	n.d.–14	n.d.–664	n.d.–275
56	Azobisisobutyronitrile, AIBN / Tetramethylsuccinonitrile, TMSN	n.d.–756	n.d.–173	n.d.–526	n.d.–216
57	N,N-Dibutylformamide	26–432	6–375	1–72	2–540
	O-containing compounds				
58	2,6-Di- <i>tert</i> -butyl-1,4-benzoquinone, BHT quinone	n.d.–10	<0.2–17	1–91	1–119
59	Butylated hydroxytoluene, BHT	1–13	1–43	1–30	1–124
60	1,3,3-Trimethyloxindole	n.d.–16	n.d.–<6	n.d.–8	n.d.–7

n.d., not detected

during wastewater treatment (Andreozzi et al., 2003; Löffler et al., 2005). Accordingly, its occurrence in aquatic systems is well studied, and the highest loads in the Rur river downstream of the WWTP Düren (population served ~94,000) were similar to those in the river Taff in Wales (up to 157 g/d) downstream of a WWTP of similar size (population served 111,000) (Kasprzyk-Hordern et al., 2008).

3.2 Riverbed

Although the sedimentary compartment, characterized by a discontinuous pollutant transport, is not as dynamic as the aqueous phase, riverbed sediments are easily mobilized and resuspended compared to areas of longer-term accumulation such as floodplains or reservoirs (Cofalla et al., 2012; Westrich & Förstner,

2007). Generally, the distribution of (suspended) particulate matter in fluvial systems is quite complex, determined by permanent ongoing processes such as accumulation, but also resuspension of particles, depending mainly on flow velocities and particle sizes (Morehead et al., 2003; Rhoads, 2020; Vercruyssen et al., 2017). As the riverbed samples were collected at a single spot close to the riverbanks, the pollution in the middle of the riverbed may be different due to higher flow velocities.

The analysis of subaquatic riverbed sediments revealed the presence of several organic pollutant groups that have already been identified in the Rur floodplains after the 2021 flood events (Schwanen et al., 2023). These include polycyclic aromatic hydrocarbons (PAHs) as indicators of petrogenic contamination, linear alkylbenzenes (LABs) as

anthropogenic markers of wastewater pollution, and polychlorinated biphenyls (PCBs) as man-made substances that were commonly used in industrial and mining applications in the past. Further on, various industrial compounds (e.g., chlorinated benzenes (Cl_2 to Cl_6), diphenoxyethane (DPE), and di-*iso*-propyl-naphthalenes (DIPNs)), but also methyltriclosan and pesticide residues such as DDE and DDD were identified. The TOC normalized amounts are summarized in Table 5. For comparison with other studies, dry weight concentrations have also been used. However, for the environmental behavior and distribution of organic contaminants, the TOC normalized amounts are more interesting as they reflect the actual environmental behavior of the substances. In addition, they show the direct risk of contaminant accumulation in organic material.

Maximum LAB amounts were similar for all sampling campaigns and ranged from 5.1 $\mu\text{g}/\text{g}_{\text{TOC}}$ (Jun. 2021) to 7.6 $\mu\text{g}/\text{g}_{\text{TOC}}$ (Nov. 2021). In general, the main contamination was found downstream of Düren (R11) correlating with the distribution of WWTPs (cf. Figure 1). In particular, in November 2021, the concentration peaks could be easily assigned to different WWTPs. The maxima were located at R12 (7.6 $\mu\text{g}/\text{g}_{\text{TOC}}$), R16 (6.3 $\mu\text{g}/\text{g}_{\text{TOC}}$), and R20 (7.4 $\mu\text{g}/\text{g}_{\text{TOC}}$) and, thus, slightly offset to the inputs of the WWTPs in Düren (R11), in Jülich/Linnich (R14 and R15) and in Aachen via the Wurm tributary (R19). This offset is probably due to the high flow velocities and dynamics during the extreme flood event in July 2021, which prevented immediate adsorption to suspended particulate matter or rather immediate sedimentation of these particles (cf. temporal effects). A possible consequence is also a remobilization of already deposited material. Overall, the concentrations were mostly lower than those found in several Asian rivers on a dry weight basis (Isobe et al., 2004; Wang et al., 2014). In particular, the average LAB contamination (between 9 and 24 $\text{ng}/\text{g}_{\text{dw}}$) was very low in the Rur river, as almost no LAB contamination was found upstream of Düren (R1 to R10). The maximum of 184 $\text{ng}/\text{g}_{\text{dw}}$ was also clearly lower than the maxima found by Isobe et al. (2004). They detected particularly high concentrations in Indonesia, Thailand, and the Philippines, with maximum values of 42.6 $\mu\text{g}/\text{g}_{\text{dw}}$, 14.1 $\mu\text{g}/\text{g}_{\text{dw}}$, and 13.0 $\mu\text{g}/\text{g}_{\text{dw}}$. These values are at least 70 times higher than the maximum value at the Rur.

The highest cumulative sum of six representative PCB congeners (PCB 28, PCB 52, PCB 101, PCB 138, PCB 153, and PCB 180) was between 8.1 $\mu\text{g}/\text{g}_{\text{TOC}}$ and 51.8 $\mu\text{g}/\text{g}_{\text{TOC}}$. In general, the individual amounts were highest for the Cl_6 - and Cl_7 -congeners, and the middle course of the Rur showed the highest PCB contamination with the maximum amounts. Specifically, the river section near Winden (R9/R10) showed a particularly high level of contamination. At R9, high summarized PCB amounts occurred in June 2021 (29.2 $\mu\text{g}/\text{g}_{\text{TOC}}$) and May 2022 (28.1 $\mu\text{g}/\text{g}_{\text{TOC}}$). Sampling campaign 3 (Nov. 2021) showed an even larger maximum at the next location R10 (51.8 $\mu\text{g}/\text{g}_{\text{TOC}}$). Again, this spatial shift is probably due to the high discharges and dynamics during the summer flood event in 2021. As the respective maxima at R9 and R10 have a similar composition, they probably originated from the same emission source. In Winden and Kreuzau, there are two paper factories as well as some metal and plastic processing companies. Partly, they discharge their wastewater effluents and precipitation water directly into the Rur river, which could be the cause of the PCB introduction. In addition, there is a reported PCB-contaminated site from a former industrial facility, which also affects the Rur river (MKULNV NRW, 2015). Considering the values based on dry weight, the ΣPCB_6 maxima were between 94 and 333 $\text{ng}/\text{g}_{\text{dw}}$. Accordingly, they were slightly lower than those of the heavily anthropogenically influenced and industrialized Huveaune river in France (up to 435 $\text{ng}/\text{g}_{\text{dw}}$), but higher than those of several Chinese rivers (Kanzari et al., 2014; Lv et al., 2015; Zhang et al., 2010).

$\Sigma\text{EPA}16$ PAHs were detected in the $\text{mg}/\text{g}_{\text{TOC}}$ —range with up to 3.3 $\text{mg}/\text{g}_{\text{TOC}}$ (Nov. 2021). Phenanthrene, fluoranthene, pyrene, chrysene, and benzo[*b*]fluoranthene accounted for the largest share of contamination. PAH maxima were distributed similarly to the maxima of PCBs, mainly in the middle course and especially in November 2021. The amounts decreased downstream of the most contaminated river section at Winden (R9/R10), but the substances were still ubiquitously present. They were also found to be ubiquitous along the Huveaune river in France (Kanzari et al., 2014). Nevertheless, the concentrations in the Rur sediments are higher with an average of 3.6 $\mu\text{g}/\text{g}_{\text{dw}}$ (mean value across all campaigns) compared to about 2 $\mu\text{g}/\text{g}_{\text{dw}}$ in the French river (Kanzari et al., 2014). The Rur mean value was also

Table 5 Span of minimum and maximum amounts [ng/g_{TOC}] of organic compounds detected in Rur riverbed samples (taken in November 2020, June 2021, November 2021, and May 2022)

No	Compounds	Detected amounts [ng/g _{TOC}]			
		Nov. 2020	Jun. 2021	Nov. 2021	May 2022
Linear alkylbenzenes, LABs					
1	Phenyldecane (C ₁₀)	n.d.–400	n.d.–220	n.d.–120	n.d.–280
2	Phenylundecane (C ₁₁)	43–2400	17–1200	5–2400	< 5–1800
3	Phenyl-dodecane (C ₁₂)	99–2900	27–2000	14–2600	6–2400
4	Phenyltridecane (C ₁₃)	120–1800	27–1900	20–3400	n.d.–2800
	Σ LABs	285–7500	72–5100	39–7620	6–6510
Polychlorinated biphenyls, PCBs					
5	Cl ₃ -PCB (PCB 28)	n.d.–2300	n.d.–1300	n.d.–1300	n.d.–780
6	Cl ₄ -PCB (PCB 52)	n.d.–690	n.d.–310	n.d.–670	n.d.–540
7	Cl ₅ -PCB (PCB 101)	n.d.–660	n.d.–2400	n.d.–4100	n.d.–2600
8	Cl ₆ -PCB (PCB 138)	13–1900	n.d.–10,000	n.d.–15,800	n.d.–8600
9	Cl ₆ -PCB (PCB 153)	9–2000	n.d.–9500	n.d.–17,200	n.d.–9900
10	Cl ₇ -PCB (PCB 180)	9–1200	n.d.–7000	n.d.–13,100	n.d.–6500
	Σ PCBs (6 representative congeners)	31–8050	93–29,175	n.d.–51,770	n.d.–28,110
Polycyclic aromatic hydrocarbons, PAHs					
11	Acenaphthylene	84–2100	36–9900	8–47,900	37–8700
12	Acenaphthene	44–3400	210–5900	17–34,800	65–10,100
13	Fluorene	86–5300	360–16,400	5–90,400	67–6600
14	Phenanthrene	2500–45,400	4800–168,000	7400–269,000	4700–172,000
15	Anthracene	370–5100	1200–43,200	1100–296,000	900–32,300
16	Fluoranthene	6300–73,300	2900–228,000	12,000–248,000	8400–143,000
17	Pyrene	4800–57,400	5200–196,000	13,500–230,000	8700–177,000
18	Benz[<i>a</i>]anthracene	2700–22,600	4900–165,000	9800–314,000	6400–141,000
19	Triphenylene/chrysene	4300–29,100	5900–196,000	15,300–328,000	8900–182,000
20	Benzo[<i>b</i>]fluoranthene	3700–27,200	10,300–303,000	22,000–623,000	13,600–282,000
21	Benzo[<i>k</i>]fluoranthene	220–1800	1100–24,700	1400–74,900	1100–35,000
22	Benzo[<i>a</i>]pyrene	1300–10,200	4400–128,000	9200–233,000	5900–147,000
23	Naphthalene	600–20,900	280–11,700	n.d.–8700	n.d.–550
24	Indeno[1,2,3- <i>cd</i>]pyrene	740–10,400	5000–113,000	8600–295,000	10,100–175,000
25	Benzo[<i>g,h,i</i>]perylene	580–6800	3800–79,800	6500–189,000	6400–130,000
26	Dibenz[<i>a,h</i>]anthracene	110–2200	1200–19,100	1400–62,600	1700–31,300
	Σ EPA16 PAHs	37,359–255,980	56,750–1,538,580	140,680–3,288,000	89,610–1,577,950
Industrial compounds					
27	Di- <i>iso</i> -propylnaphthalenes, DIPNs	16–6200	n.d.–8300	< 5–33,000	n.d.–11,800
28	Diphenoxyethane, DPE	n.d.–120	n.d.–260	n.d.–2200	n.d.–140
29	Mesamoll®	n.d.–310	n.d.–7900	n.d.–1900	n.d.–3500
30	Butylated hydroxytoluene, BHT	n.d.–78	n.d.–130	n.d.–120	n.d.–320
31	Dichlorobenzenes (Cl ₂)	n.d.–498	n.d.–64	n.d.–329	n.d.–161
32	Trichlorobenzenes (Cl ₃)	n.d.–247	n.d.–24	n.d.–117	n.d.–62
33	Tetrachlorobenzenes (Cl ₄)	n.d.–11	n.d.	n.d.	n.d.–< 5
34	Pentachlorobenzene (Cl ₅)	n.d.–< 5	n.d.–< 5	n.d.	n.d.–< 5
35	Hexachlorobenzene (Cl ₆)	n.d.–10	n.d.–< 5	n.d.	n.d.–< 5
	Σ Chlorinated benzenes (Cl ₂ to Cl ₆)	n.d.–756	n.d.–81	n.d.–446	n.d.–210
Pesticide residues					

Table 5 (continued)

No	Compounds	Detected amounts [ng/g _{TOC}]			
		Nov. 2020	Jun. 2021	Nov. 2021	May 2022
36	Dichlorodiphenyldichloroethylene, DDE	n.d.–180	n.d.–180	n.d.–29	n.d.–120
37	Dichlorodiphenyldichloroethane, DDD	n.d.–10,930	n.d.–630	n.d.–990	n.d.–940
	Σ DDX	n.d.–10,944	n.d.–681	n.d.–990	n.d.–1060
	Personal care products				
38	Methyltriclosan	n.d.–160	n.d.–64	n.d.–46	n.d.–36
39	Octocrylene	n.d.	n.d.–27	n.d.	n.d.–32

n.d., not detected

higher than that of several Chinese rivers (e.g., Licun river, Yang river, and Dagu river), but similar to that of the Moshui (\emptyset 4 $\mu\text{g/g}_{\text{dw}}$) and the Daliao river (\emptyset 3.7 $\mu\text{g/g}_{\text{dw}}$) in China, and the Prai river (\emptyset 4.4 $\mu\text{g/g}_{\text{dw}}$) in Malaysia (Han et al., 2021; Keshavarzifard et al., 2014; Zheng et al., 2016). According to Net et al. (2015), there are also several French rivers that show an even higher contamination, with average values of 6.4 $\mu\text{g/g}_{\text{dw}}$ (Senseé river), 9.9 $\mu\text{g/g}_{\text{dw}}$ (Deûle river), and 20.7 $\mu\text{g/g}_{\text{dw}}$ (Scarpe river).

Furthermore, DIPNs were the most frequently detected industrial compounds with the highest amounts ranging from 6.2 $\mu\text{g/g}_{\text{TOC}}$ (Nov. 2020) to 33.0 $\mu\text{g/g}_{\text{TOC}}$ (Nov. 2021). As many other organic pollutants, they occurred in high amounts downstream of Düren. However, these amounts on a dry weight basis (max. 310 ng/g_{dw}) were much lower than in various Indonesian river sediments (max. 16,000 ng/g_{dw}), but still higher than in the meso-scaled Lippe river (max. 83 ng/g_{dw}) and the macro-scaled Rhine river (max. 61 ng/g_{dw}) in Germany (Dsikowitzky et al., 2020; Franke et al., 2007).

3.3 Temporal Effects

Time is a crucial factor in the fate and behavior of organic pollutants in our environment. Some substances are rapidly degraded, while others remain stable in different compartments for long periods of time. Partly, they are very persistent or form transformation products. However, time is also critical for transport and accumulation, as some phases are more dynamic than others, river systems undergo annual changes, and extreme events such as heavy rainfall, storms, or floods

can lead to increased remobilization (e.g., Crawford et al., 2022; Förstner, 2004; La Farré et al., 2008).

Temporal variations of the highly dynamic aqueous phase over a longer period of time (2004 to 2020) have already been investigated in a previous study (Schwanen & Schwarzbauer, 2022). Nevertheless, even in the shorter period of this study when more regular, monitoring-like sampling was conducted, general trends in the emission profiles were recognizable for some substances (cf. Figure 2).

For instance, a steady increase in tocopheryl acetate loads was observed (up to 48 g/d in November 2020 and up to 1355 g/d in May 2022), which is likely to be associated with higher consumption. Additionally, the contamination with DPE and other industrial substances such as triethylcitrate and acetyl tributylcitrate increased from 2020 to 2022, especially in the urbanized lowland part (cf. Figure 2). In contrast, slight decreases were recognizable for some substances such as the pharmaceutical oxcarbazepine or tetraacetylenediamine (TAED), a bleaching activator in laundry detergents. This could be due to a reduced use or an improved wastewater treatment, as for the latter this trend was already clearly visible in an earlier, longer period from 2004 to 2020 (Schwanen & Schwarzbauer, 2022).

Such longer-term developments or trends are essentially determined by external factors (e.g., changes in consumer behavior or improved treatment processes in WWTPs). These factors may also lead to seasonal differences in the contamination situation. However, there may also be other reasons for seasonality, such as (natural) degradation and transformation processes in the river. The emission

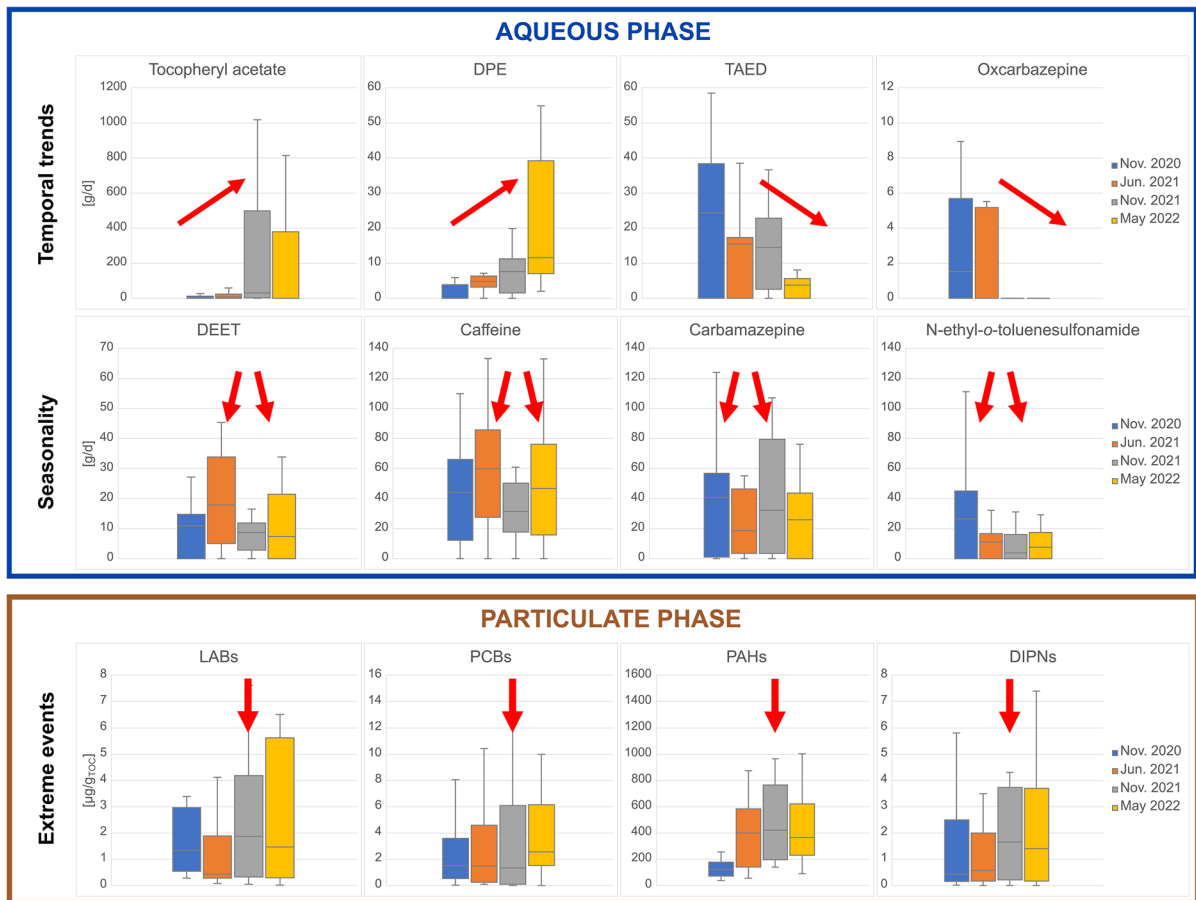


Fig. 2 Box and Whisker plot of the loads and amounts of selected xenobiotic organic pollutants in the aqueous and particulate (riverbed) phase of the Rur river in November 2020 (blue), June 2021 (orange), November 2021 (gray), and May 2022 (yellow)

profiles and the comparison of the annual patterns can give some indication in this context. Important questions are whether the amounts or loads introduced into the river system were comparable in summer and winter, whether consumption quantities varied and whether the substance degraded rapidly immediately after its introduction or not. Due to the higher dynamics of the aqueous phase compared to the sedimentary phase, seasonal phenomena are particularly expected in this compartment.

In the Rur river, many substances in the watery phase showed a seasonal behavior. These were mainly physiologically active substances (e.g., the pharmaceuticals carbamazepine and lidocaine), but industrial compounds (e.g., triphenylphosphine oxide) and naturally occurring substances (e.g., coumarin) were also identified with specific distribution patterns.

The seasonal behavior of carbamazepine has already been addressed in several studies (Fernández et al., 2014; Golovko et al., 2014; Lindholm-Lehto et al., 2016). Although its removal efficiency and bi- and photodegradation potential are very low throughout the entire year (Andreozzi et al., 2003; Fernández et al., 2014; Löffler et al., 2005; Matamoros et al., 2009), seasonal differences have been observed, showing a higher level of pollution during the winter months (see Fig. 2). As carbamazepine is also used in the treatment of depression and mania or in alcohol withdrawal, Lindholm-Lehto et al. (2016) and Matamoros and Salvadó (2012) suspect a higher consumption during the winter months due to an increased use of psychotropic drugs.

Consumption patterns are also likely to explain the observed seasonal variations of caffeine and

N,N-diethyl-*m*-toluamide (DEET). In contrast to carbamazepine, these two substances had higher loads in summer. As DEET is mainly used as an insect repellent, extended application during the summer insect season is likely (Quednow & Püttmann, 2009). Recreational use may be a reason for the seasonal differences of the psychoactive substance and stimulant caffeine, as higher summer loads were also reported in Greek and Polish rivers, due to higher human consumption as a result of longer periods of daylight and increased human activity (Jagoda et al., 2015; Kosma et al., 2010). Removal efficiencies in WWTPs are generally high (> 99%) and not seasonal dependent (Buerge et al., 2003; Fernández et al., 2014). Yet, there were larger fluctuations in the summer emission profiles. In winter, the loads remained quite high after caffeine introduction, i.e., there was only a minor degradation. In summer, there was typically a rapid decline and much lower loads at the subsequent sites. This could be due to increased bioactivity or other degradation processes (Buerge et al., 2003; Lam et al., 2004). For instance, Buerge et al. (2003) demonstrated that biodegradation and especially photodegradation of caffeine was more effective in mid-summer under clear skies.

N-Ethyltoluenesulfonamides (NETSA) are used as plasticizers in resins, coatings, adhesives, and printing inks (e.g., Štěpek & Daoust, 1983). In the Rur catchment, food packaging factories are a likely emission source, probably requiring the same quantities for production throughout the year (Alexander et al., 2008; Skjevraak et al., 2005). However, the maximum loads of N-ethyl-*o*-toluenesulfonamide were noticeably higher in winter (Nov. 2020: 111 g/d and Nov. 2021: 66 g/d) than in summer (Jun. 2021: 32 g/d and May 2022: 49 g/d). This is likely due to a lower treatment performance of the WWTPs in winter, although precise data on removal efficiencies are lacking. Sui et al. (2011) have shown that the removal of pharmaceuticals and personal care products by conventional activated sludge as biological treatment process (as it is the case for most of the WWTPs in the catchment) varies throughout the year. Possibly, this difference in efficiency is similar for industrial compounds.

When looking at the minimum and maximum amounts in Table 5 and the corresponding emission profiles, it is immediately apparent that seasonality does not play a major role for the contaminants detected in the sedimentary phase. This result was

to be expected due to the lower dynamics of this compartment and the typically higher persistence of lipophilic substances. Occasionally, octocrylene was found in summer sampling campaigns. The associated emission profiles thus showed a certain degree of seasonality, probably due to consumption behavior, as octocrylene is still used commercially in sunscreen products (Schneider & Lim, 2019). However, the amounts were very low (up to 27 ng/g_{TOC} in June 2021 and 32 ng/g_{TOC} in May 2022).

Nevertheless, a remarkable change in the sediment contamination due to an extreme flood event in July 2021 was evident (Schwanen et al., 2023). Amounts before this flood were, for the most part, considerably lower than afterwards. In particular, the November 2021 sampling campaign showed several extreme maxima and more severe contamination along the entire river course. This was particularly evident for LABs, PCBs, and PAHs, but also for industrial substances such as DIPNs (cf. Figure 2).

On average, the sum of LABs (C₁₀–C₁₃) was 1.9 µg/g_{TOC} in November 2020, 1.3 µg/g_{TOC} in June 2021, 2.6 µg/g_{TOC} in November 2021, and 2.5 µg/g_{TOC} in May 2022. Thus, a clear difference in contamination before and after the extreme flood in July 2021 was observed. The amounts in November 2021 and May 2022 were comparable and mostly even higher than those detected at the Rur floodplains in July 2021. Thus, the majority of the flood-induced LAB contamination remained in the immediate riverbed, which is important for further risk assessment as there is only a minor washing out but a clear enrichment in the river itself.

For the pollutant groups of PCBs, PAHs, and DIPNs, the difference between riverbed and floodplain amounts is even more pronounced (see Table 6). In November 2021 (sampling campaign 3), the highest sum of six representative PCB congeners was 51.8 µg/g_{TOC}. This value is almost 4 times higher than the flood-maximum of 13.7 µg/g_{TOC} at the corresponding floodplain in July 2021. Generally, the PCB contamination was highest in November 2021 with an average of 5.7 µg/g_{TOC} compared to the values of November 2020 (2.2 µg/g_{TOC}), June 2021 (4.1 µg/g_{TOC}), and May 2022 (4.9 µg/g_{TOC}). The modest increase from November 2020 to June 2021 could be due to a smaller winter flood in late January/early February 2021, while the large increase from June to November 2021 is most likely due to the extreme

Table 6 Comparison of maximum amounts [$\mu\text{g}/\text{g}_{\text{TOC}}$] of organic compounds detected in Rur riverbed samples (taken in November 2021) and floodplain samples (taken immediately after the flood event in July 2021, cf. Schwanen et al. (2023))

Pollutant (group)	Maximum amounts [$\mu\text{g}/\text{g}_{\text{TOC}}$]	
	Riverbed	Floodplain
Σ LABs	7.6	4.4
Σ EPA16 PAHs	3300	500
Σ PCB6	51.8	13.7
DIPNs	33	14.2
DPE	2.2	0.8

flood in July 2021 (Schwanen et al., 2023). The trend is also very similar for the pollutant groups of PAHs and DIPNs showing a clear difference in contamination before and after the summer flood. Again, for both groups, the amounts in November 2021 were much higher than in the adjacent floodplains in July 2021.

3.4 Spatial Effects

Besides the temporal aspect, the spatial distribution and, particularly, the range of contaminants within different compartments of a river system are of crucial importance for risk assessment and pollutant mitigation. Distribution ranges can be identified based on the emission profiles of various marker substances and the location of the corresponding emission sources. Along the Rur, the latter are mainly located in the northern, lowland part and can be traced back to urban and industrial applications. Depending on the different dynamics of the river compartments as well as the persistence and stability of the substances, longer transport distances and thus a greater range can be assumed.

For both, the aqueous and sedimentary phases, the main contamination with organic compounds occurred in the middle to lower reaches of the Rur. The input of substances due to WWTPs, particularly those in Düren, Jülich, Linnich, and Aachen (the latter discharging into the Wurm tributary), plays a decisive role. Most of the WWTPs in the Rur catchment treat both municipal and industrial influents, showing a diverse xenobiotic contamination. However, the WWTP Düren (R11) is the main emitter of most of the identified compounds. It is the largest WWTP in

the catchment area discharging directly into the Rur river, with an annual treated wastewater volume of 21 million m^3 (Wasserverband Eifel-Rur, 2017c). Accordingly, the contamination is generally higher downstream of Düren, in the urban part of the catchment system, than in the more natural Eifel region.

For example, this influence is very clear in the case of the already mentioned hydrophilic, industrial substances N-ethyl-*o*-toluenesulfonamide and azobisisobutyronitrile (AIBN) respectively its degradation product tetramethylsuccinonitrile (TMSN). They were detected almost exclusively in the urban and industrial part of the Rur catchment, starting downstream of the discharge location of the WWTP Düren. This is also where the maximum loads were found. Although the loads decrease immediately after the sampling location R11, they remain at a quite constant level from this point onwards, indicating a specific stability of these compounds (cf. Schwanen & Schwarzbauer, 2022).

In general, the emission patterns are similar for most of the identified contaminants in the aqueous phase. Looking at the total water contamination as shown in Fig. 3, sampling location R11 immediately downstream of the WWTP Düren is of outstanding relevance. Afterward, the overall load remains at a high, almost constant level. In fact, most of the substances identified in the river water show relative persistence and stability and are even transported to the superior river system throughout the year. Similar emission patterns for several organic pollutants have also been identified in the Lippe river, which is a meso-scaled tributary of the Rhine river (Dzikowitzky et al., 2004). In contrast, the Rhine river itself shows a more variable and dynamic contamination due to multiple emission sources and inflowing meso-scaled tributaries (Schwarzbauer & Heim, 2005). Range and transport of different contaminants therefore varies depending on the size and dimension of the river system and the corresponding flow patterns and discharges. Further information on specific environmental behaviors and emission characteristics in this compartment can be found in Schwanen and Schwarzbauer (2022).

As for the river water, the main contamination of the riverbed compartment occurred in the middle to lower reaches of the Rur, with the point source WWTP Düren (R11) having a major impact. Especially in November 2021, high amounts were

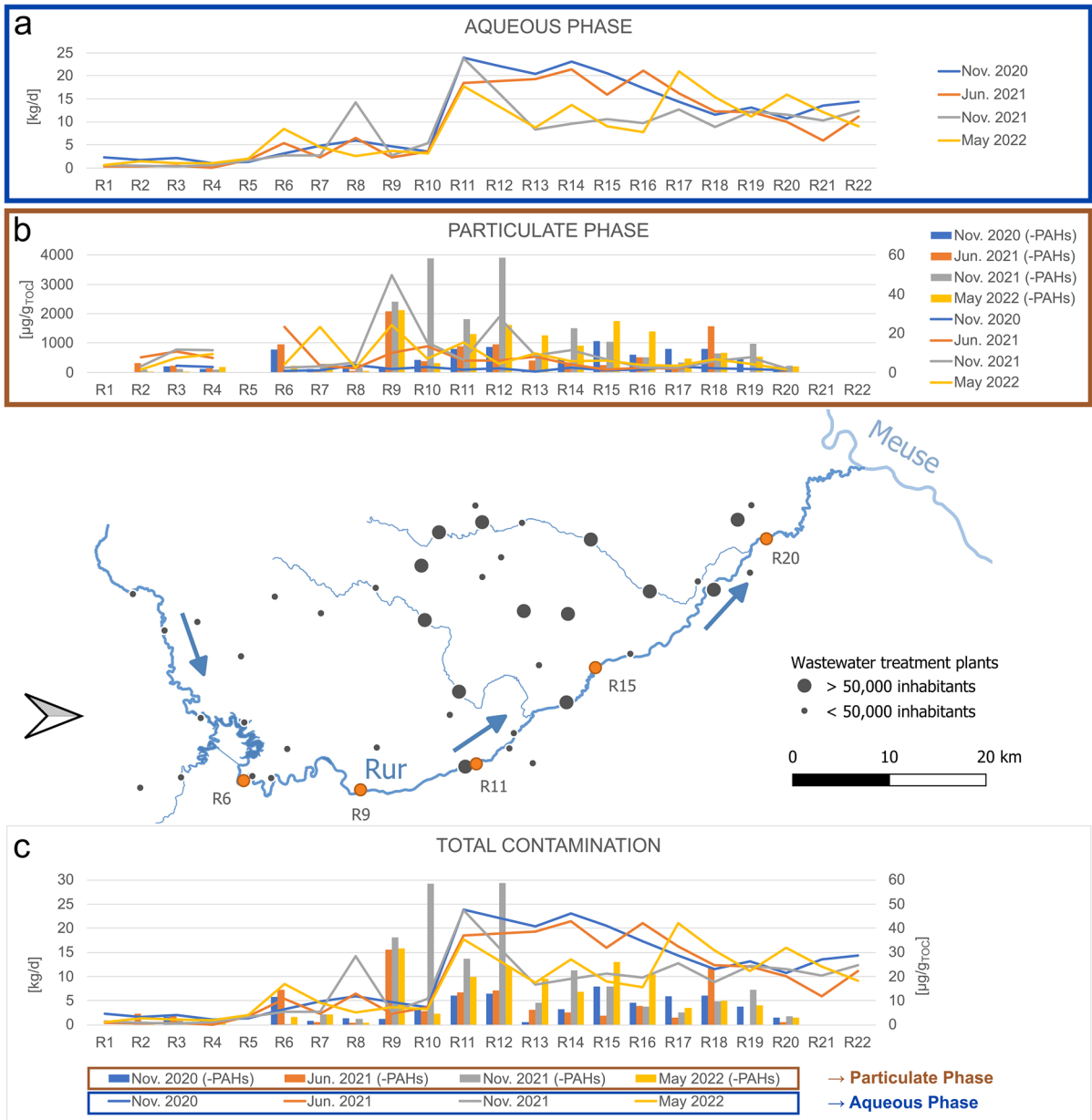


Fig. 3 Spatial and temporal distribution of xenobiotic organic contaminants in different phases of the Rur river in November 2020 (blue), June 2021 (orange), November 2021 (gray), and May 2022 (yellow). **a** Shows the total aqueous contamination as a sum of the compounds in Table 4. **b** Shows the total sedimentary contamination as a sum of the compounds in Table 5

with (lines, primary axis) and without (bars, secondary axis) the amounts of Σ EPA16 PAHs. No sediment samples could be taken at locations R1, R5, R21, and R22. **c** Combines the total contamination of both phases (lines: aqueous contamination; bars: particulate contamination (without PAHs))

detected at this river section. However, the maxima were shifted slightly downstream, probably due to high flood discharges in the summer of 2021 (cf. temporal effects). Instead of having amount maxima

at sampling location R11, i.e., immediately downstream of the WWTP, high amounts were detected 4 km further downstream at R12 (Schophoven). A weir located at this sampling location dams up the

river reduces the flow velocity and presumably leads to an increased sedimentation of suspended particles. In particular, LABs as wastewater indicator were detected at this site.

In general, the sampling campaign of November 2021 shows a higher contamination with peak values not only downstream of the WWTP Düren at Schophoven (R12) but also at Üdingen/Winden (R9/10). The emission profiles for the other sampling campaigns are similar. The total contamination (lines in Fig. 3b) is generally dominated by high PAH amounts, so that it looks almost identical to the corresponding PAH emission profile. PAHs are ubiquitously present and often originate from diffuse sources. Therefore, the total contamination without PAHs is also visible as bars, showing a slight shift of the first maximum from R9 to R10 as well as a greater contamination difference between the upper and lower course of the river. Thus, the results indicate a specific dynamic transport of the riverbed sediment and the associated pollution, probably even reaching the superordinate river system.

Finally, although the contaminants are not the same in the different compartments, the pollution situation and emission patterns are comparable. Main emission sources are located in the industrial and urban centers, and the pollutant inputs are mainly from the corresponding WWTP effluents. The overall contamination profiles of the riverbed and the river water are very similar, especially when the ubiquitous group of PAHs is subtracted (see Fig. 3c). Both compartments contribute to a dynamic contaminant input into the superior river system of the Meuse. Therefore, the transport and range of hydrophilic and lipophilic pollutants within this catchment system appears to be closely connected. Nevertheless, the input of the respective contaminants is slightly different. In the case of the sedimentary phase, the maximum contamination results not only from the inputs from municipal WWTPs but also from industrial direct dischargers. Downstream of the main emissions in the middle reaches, the pollution decreases clearly but remains at a much higher level than in the near-natural Eifel region. The difference between these two regions is even more pronounced in the highly dynamic aqueous phase. Thus, the distribution ranges of contaminants for both phases clearly exceed the dimension of a meso-scaled river system and need to be considered

in risk and hazard assessments of superior, macro-scaled river systems.

3.5 Limiting Factors

In particular, the transport of lipophilic pollutants is closely linked to the transport of suspended particulate matter. However, most river systems are strongly influenced by anthropogenic measures and regulations. Meso-scaled rivers such as the Rur are often regulated by a single or even a chain of larger dams. Furthermore, channelization and the construction of, e.g., weirs are typical anthropogenic measures (Petts, 1999). These can therefore provide restrictions on the transport and range of pollutants. As shown above, the main pollutant transport of the two investigated phases seems to be closely connected in the middle and lower reaches of the Rur, despite the presence of weirs and channelization within this part of the river.

Yet, the largest anthropogenic regulation in the Rur catchment is the system of dams in the mountainous landscape of the Eifel. The corresponding reservoirs are used for flood protection, energy generation, drinking water supply, and also for recreational purposes, among other things (Wasserverband Eifel-Rur, 2017d). Therefore, this river section was focused on to determine the anthropogenic influence on the transport of pollutants and on the close connection of the aqueous and particulate phases (cf. spatial effects). Reservoirs are located between R4 and R6 (“Rurtalsperre”) and between R8 and R9 (“Obermaubach basin”). Sampling site R5 is located within the dam system of the Rurtalsperre and only water sampling could be performed at this location.

In general, the Rurtalsperre is one of the largest reservoirs in Germany with a storage volume of 202.6 million m³ of water (Wasserverband Eifel-Rur, 2017a). In contrast, the Obermaubach basin is much smaller with a storage capacity of only 1.65 million m³ (Wasserverband Eifel-Rur, 2017b). As shown by Wolf et al. (2022), both of them function as sinks for suspended particulate matter and accumulated inorganic pollutants (Cu and Pb). Thus, they are also expected to be a major sink for lipophilic organic pollutants and to have a strong influence on the sedimentary pollutant transport.

In November 2020, the total riverbed contamination as the sum of all substances in Table 5 was generally low in the Eifel region. Nevertheless,

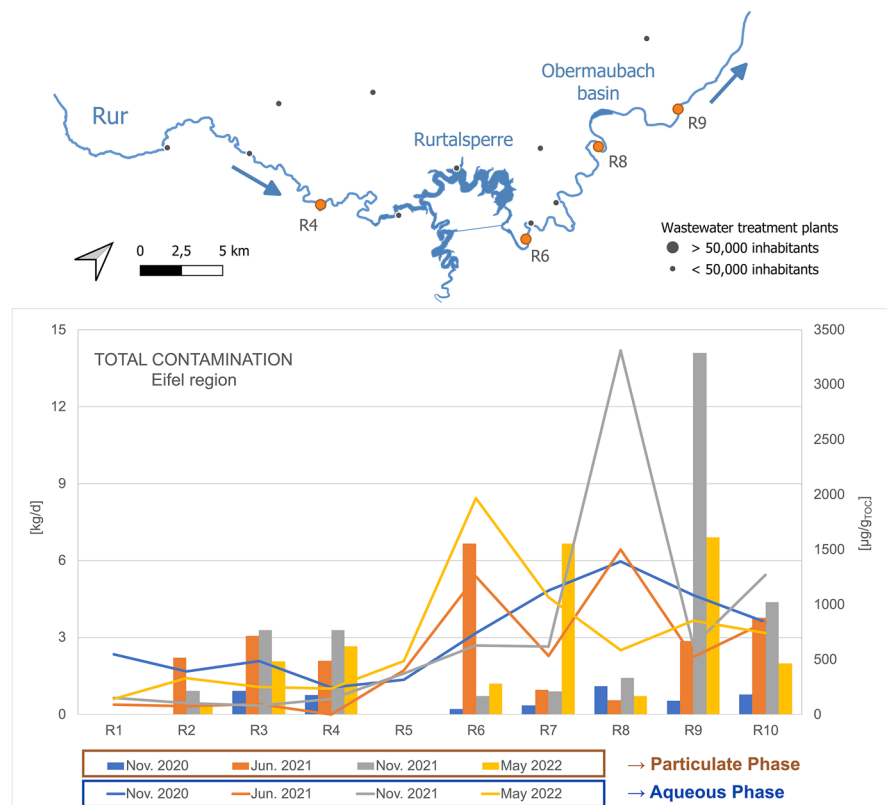
the influence of the reservoirs was recognizable in the overall emission profile (see Fig. 4). The total amounts were higher before than after the reservoir (R4 177.7 $\mu\text{g}/\text{g}_{\text{TOC}}$ vs. R6 49.9 $\mu\text{g}/\text{g}_{\text{TOC}}$ and R8 258.6 $\mu\text{g}/\text{g}_{\text{TOC}}$ vs. R9 125.4 $\mu\text{g}/\text{g}_{\text{TOC}}$). This is attributed to the sediment retention in the reservoirs, which greatly reduces the amount of suspended and fine particulate matter, resulting in a sediment deficit downstream of the dams (Dai & Liu, 2013; Schmidt & Wilcock, 2008; Wolf et al., 2022). However, the situation is different for the following sampling campaigns. In June 2021, the amounts downstream of the reservoirs were higher than at the previous sampling locations. In fact, the maximum of the entire sampling campaign was detected at R6 downstream of the Rurtalsperre (1.6 $\text{mg}/\text{g}_{\text{TOC}}$). At the end of January/beginning of February 2021, there was a smaller flood event in this river system, which may have led to a remobilization of fine sediments and associated pollutants deposited in the reservoirs (cf. Schwanen et al., 2023). Similarly, the extreme flood in July 2021 is likely to have caused remobilization of reservoir sediments. In November 2021, the highest overall

maximum was detected at R9 downstream of the Obermaubach basin (3.3 $\text{mg}/\text{g}_{\text{TOC}}$). This maximum was still recognizable in May 2022, but due to further transport and remobilization, the contamination level had already decreased again (1.6 $\text{mg}/\text{g}_{\text{TOC}}$).

In contrast, no contaminant retention by the reservoirs could be identified for the aqueous phase. Instead, the Rurtalsperre was an additional emission source in the catchment system due to its recreational usage (such as camping, passenger shipping, sailing, swimming, and other water sport activities). In summer months (sampling campaigns 2 and 4), the stimulant caffeine was detected with increased loads downstream of the reservoir (cf. temporal effects). Additionally, load peaks of the fragrance dihydro-methyljasmonate were detected at the corresponding sampling location.

Overall, the dam system results in a disconnection of the dynamic contaminant transport in the aqueous and particulate phases, highlighting the anthropogenic influence not only on the emission but also on the transport and thus the range of different pollutants. Nevertheless, there are also several

Fig. 4 Spatial and temporal distribution of xenobiotic organic contaminants in the aqueous and particulate (riverbed) phase of the Rur river in the near-natural Eifel region in November 2020 (blue), June 2021 (orange), November 2021 (gray), and May 2022 (yellow). The respective total contamination is the sum of the compounds in Tables 4 and 5 (without the amounts of $\Sigma\text{EPA16 PAHs}$). Reservoirs are located between R4 and R6 (“Rurtalsperre”) as well as between R8 and R9 (“Obermaubach basin”)



other anthropogenic measures that affect the sediment budget and possibly lead to a sediment excess or deficit. These include changes in land use (e.g., due to deforestation or sealing), but also renaturation measures (Maaß et al., 2018; Vercruyssen et al., 2017; Vörösmarty et al., 2003). The latter could also contribute to the creation of sediment and pollutant sinks. However, small renaturalized areas in the middle and lower reaches of the Rur river (e.g., at Körrenzig near R16) had no influence on sediment transport and did not lead to a disconnection of particulate and aqueous phases. The situation was similar for weirs and straightened sections. Thus, a decoupling of the dynamic pollution transport from different compartments is likely to occur only in the case of large-scale anthropogenic measures with at least regional influence.

4 Conclusions

This study investigated the accumulation, transport, and fate of organic pollutants in different dynamic compartments of the Rur river over a period of four bi-annual sampling campaigns. Using the example of the Rur river, some generally valid statements regarding the contamination of the river water as well as the riverbed could be proven:

- **Temporal effects:** Temporal effects occur in different dimensions for both the aqueous and particulate phases within a river system. For the more dynamic water phase, mainly regular, seasonal effects can be identified, while the transport of riverbed sediment and the accumulated pollutants is mainly determined by exceptional events, such as heavy rainfall and floods. Interestingly, after an extreme flood event, the amounts found in the riverbed were mostly higher than on the adjacent floodplains
- **Spatial effects:** The main emission sources are comparable for the aqueous and sedimentary phases. WWTPs, and thus associated industrial and urban effluents (especially from the paper industry), are mainly responsible for the peak loads and amounts. In addition to direct discharges, indirect discharges resulting from surface runoff and flooding are also of great relevance for sedimentary pollution. Both compart-

ments show a high, almost constant contamination level after the main input in the more urban part of the catchment system and consequently a similar range of pollutant transport. Thus, both lipophilic and hydrophilic substances contribute to the contamination of the superior river

- **Limiting factors:** Anthropogenic regulations such as weirs, dams, and channelization have a major impact on the transport of pollutants associated with the particulate but not the aqueous compartment. Reservoirs in particular act as temporary sinks for lipophilic pollutants but sediments can be remobilized during flood events and increased discharges

Overall, this study provides a good overview of the different triggers and factors that influence the distribution, fate, and accumulation of hydrophilic and lipophilic contaminants in a river system. Although there is some slight temporal and spatial heterogeneity, pollutant transport in the aqueous and particulate phases is closely connected. The complementary investigation of the different phases in a river system has only been done in a few studies. However, this combined approach is an important aspect for a comprehensive view of environmental contamination. Therefore, the general approach and implications investigated in this study can be transferred and applied to other anthropogenically influenced river systems. The consideration of multiple phases and different triggers or key drivers is the first crucial step for risk assessment and, more importantly, for subsequent pollutant mitigation and reduction.

Acknowledgements Special thanks to the support of Mrs. Yvonne Esser and Mrs. Annette Schneiderwind during laboratory work. In addition, C.S. thanks the RWTH Scholarships for Doctoral Students.

Funding Open Access funding enabled and organized by Projekt DEAL. C.S. was financially supported by the RWTH Aachen University Scholarships for Doctoral Students.

Data Availability All data generated or analyzed during this study are included in this published article and its supplementary information files.

Declarations

Competing Interests The authors declare no competing interests.

Open Access This article is licensed under a Creative Commons Attribution 4.0 International License, which permits use, sharing, adaptation, distribution and reproduction in any medium or format, as long as you give appropriate credit to the original author(s) and the source, provide a link to the Creative Commons licence, and indicate if changes were made. The images or other third party material in this article are included in the article's Creative Commons licence, unless indicated otherwise in a credit line to the material. If material is not included in the article's Creative Commons licence and your intended use is not permitted by statutory regulation or exceeds the permitted use, you will need to obtain permission directly from the copyright holder. To view a copy of this licence, visit <http://creativecommons.org/licenses/by/4.0/>.

References

- Aachener, Z. (2021). *Das weltbekannte Blütenpapier aus Zerkall ist Geschichte*. Aachener Zeitung. Retrieved December 4, 2023, from https://www.aachener-zeitung.de/lokales/dueren/huertgenwald/das-weltbekanntebuettenpapier-aus-zerkall-ist-geschichte_aid-64607993
- Alexander, J., Binderup, M.-L., Dahl, K.H., Hetland, R.B., Husøy, T., Paulsen, J.E., Sanner, T., Steffensen, I.-L., & Thrane, V. (2008). *Opinion of the scientific panel on food additives, flavourings, processing aids, materials in contact with food and cosmetics of the Norwegian Scientific Committee for Food Safety. Risk assessment of N-ethyltoluenesulfonamide (NETSA) used as plasticizer in printing inks on food packaging materials*. VKM Report.
- Andreozzi, R., Raffaele, M., & Nicklas, P. (2003). Pharmaceuticals in STP effluents and their solar photodegradation in aquatic environment. *Chemosphere*, *50*(10), 1319–1330. [https://doi.org/10.1016/S0045-6535\(02\)00769-5](https://doi.org/10.1016/S0045-6535(02)00769-5)
- Bährle-Rapp, M. (2007). *Springer Lexikon Kosmetik und Körperpflege* (German). Springer.
- Bernhardt, E. S., Rosi, E. J., & Gessner, M. O. (2017). Synthetic chemicals as agents of global change. *Frontiers in Ecology and the Environment*, *15*(2), 84–90. <https://doi.org/10.1002/fee.1450>
- Best, J. (2019). Anthropogenic stresses on the world's big rivers. *Nature Geoscience*, *12*(1), 7–21. <https://doi.org/10.1038/s41561-018-0262-x>
- Buerge, I. I., Poiger, T., Müller, M. D., & Buser, H.-R. (2003). Caffeine, an anthropogenic marker for wastewater contamination of surface waters. *Environmental Science & Technology*, *37*(4), 691–700. <https://doi.org/10.1021/es020125z>
- Cofalla, C., Hudjetz, S., Roger, S., Brinkmann, M., Frings, R., Wölz, J., Schmidt, B., Schäffer, A., Kammann, U., Hecker, M., Hollert, H., & Schüttrumpf, H. (2012). A combined hydraulic and toxicological approach to assess re-suspended sediments during simulated flood events—Part II: An interdisciplinary experimental methodology. *Journal of Soils and Sediments*, *12*(3), 429–442. <https://doi.org/10.1007/s11368-012-0476-2>
- Crawford, S. E., Brinkmann, M., Ouellet, J. D., Lehmkuhl, F., Reicherter, K., Schwarzbauer, J., Bellanova, P., Letmathe, P., Blank, L. M., Weber, R., Brack, W., van Dongen, J. T., Menzel, L., Hecker, M., Schüttrumpf, H., & Hollert, H. (2022). Remobilization of pollutants during extreme flood events poses severe risks to human and environmental health. *Journal of Hazardous Materials*, *421*, 126691. <https://doi.org/10.1016/j.jhazmat.2021.126691>
- Dai, Z., & Liu, J. T. (2013). Impacts of large dams on downstream fluvial sedimentation: An example of the Three Gorges Dam (TGD) on the Changjiang (Yangtze River). *Journal of Hydrology*, *480*, 10–18. <https://doi.org/10.1016/j.jhydrol.2012.12.003>
- Dsikowitzky, L., Schwarzbauer, J., & Littke, R. (2002). Distribution of polycyclic musks in water and particulate matter of the Lippe River (Germany). *Organic Geochemistry*, *33*(12), 1747–1758. [https://doi.org/10.1016/S0146-6380\(02\)00115-8](https://doi.org/10.1016/S0146-6380(02)00115-8)
- Dsikowitzky, L., Schwarzbauer, J., & Littke, R. (2004). The anthropogenic contribution to the organic load of the Lippe River (Germany). Part I: Quantification of specific organic contaminants. *Chemosphere*, *57*(10), 1289–1300. <https://doi.org/10.1016/j.chemosphere.2004.08.053>
- Dsikowitzky, L., Botalova, O., Illgut, S., Bosowski, S., & Schwarzbauer, J. (2015). Identification of characteristic organic contaminants in wastewaters from modern paper production sites and subsequent tracing in a river. *Journal of Hazardous Materials*, *300*, 254–262. <https://doi.org/10.1016/j.jhazmat.2015.07.001>
- Dsikowitzky, L., Hagemann, L., Dwiytmo Ariyani, F., Irianto, H. E., & Schwarzbauer, J. (2017). Complex organic pollutant mixtures originating from industrial and municipal emissions in surface waters of the megacity Jakarta—An example of a water pollution problem in emerging economies. *Environmental Science and Pollution Research*, *24*(35), 27539–27552. <https://doi.org/10.1007/s11356-017-0164-2>
- Dsikowitzky, L., Crawford, S. E., Nordhaus, I., Lindner, F., Dwiytmo Irianto, H. E., Ariyani, F., & Schwarzbauer, J. (2020). Analysis and environmental risk assessment of priority and emerging organic pollutants in sediments from the tropical coastal megacity Jakarta. *Indonesia. Regional Studies in Marine Science*, *34*, 101021. <https://doi.org/10.1016/j.rsma.2019.101021>
- Eganhouse, R. P., & Kaplan, I. R. (1985). alpha-Tocopheryl acetate as an indicator of municipal waste contamination in the environment. *Environmental Science & Technology*, *19*(3), 282–285. <https://doi.org/10.1021/es00133a014>
- Ekka, A., Pande, S., Jiang, Y., & van der Zaag, P. (2020). Anthropogenic modifications and river ecosystem services: A landscape perspective. *Water*, *12*(10), 2706. <https://doi.org/10.3390/w12102706>
- Esser, V., Buchty-Lemke, M., Schulte, P., Podzun, L. S., & Lehmkuhl, F. (2020). Signatures of recent pollution profiles in comparable central European rivers – Examples from the international River Basin District Meuse. *CATENA*, *193*, 104646. <https://doi.org/10.1016/j.catena.2020.104646>
- Fernández, M., Fernández, M., Laca, A., Laca, A., & Díaz, M. (2014). Seasonal occurrence and removal of

- pharmaceutical products in municipal wastewaters. *Journal of Environmental Chemical Engineering*, 2(1), 495–502. <https://doi.org/10.1016/j.jece.2014.01.023>
- Ferreira da Silva, B., Jelic, A., López-Serna, R., Mozeto, A. A., Petrovic, M., & Barceló, D. (2011). Occurrence and distribution of pharmaceuticals in surface water, suspended solids and sediments of the Ebro river basin. *Spain. Chemosphere*, 85(8), 1331–1339. <https://doi.org/10.1016/j.chemosphere.2011.07.051>
- Förstner, U. (2004). Sediment dynamics and pollutant mobility in rivers: An interdisciplinary approach. *Lakes & Reservoirs: Science, Policy and Management for Sustainable Use*, 9(1), 25–40. <https://doi.org/10.1111/j.1440-1770.2004.00231.x>
- Franke, S., Grunenber, J., & Schwarzbauer, J. (2007). The isomer-specific analysis of di-iso-propylnaphthalenes. *International Journal of Environmental Analytical Chemistry*, 87(6), 437–448. <https://doi.org/10.1080/03067310601025221>
- Gandy, C. J., Smith, J. W. N., & Jarvis, A. P. (2007). Attenuation of mining-derived pollutants in the hyporheic zone: A review. *Science of the Total Environment*, 373(2–3), 435–446. <https://doi.org/10.1016/j.scitotenv.2006.11.004>
- Golovko, O., Kumar, V., Fedorova, G., Randak, T., & Grabic, R. (2014). Seasonal changes in antibiotics, antidepressants/psychiatric drugs, antihistamines and lipid regulators in a wastewater treatment plant. *Chemosphere*, 111, 418–426. <https://doi.org/10.1016/j.chemosphere.2014.03.132>
- Han, B., Liu, A., Gong, J., Li, Q., He, X., Zhao, J., & Zheng, L. (2021). Spatial distribution, source analysis, and ecological risk assessment of polycyclic aromatic hydrocarbons (PAHs) in the sediments from rivers emptying into Jiaozhou Bay, China. *Marine Pollution Bulletin*, 168, 112394. <https://doi.org/10.1016/j.marpolbul.2021.112394>
- Heim, S., Schwarzbauer, J., Kronimus, A., Littke, R., Woda, C., & Mangini, A. (2004). Geochronology of anthropogenic pollutants in riparian wetland sediments of the Lippe River (Germany). *Organic Geochemistry*, 35(11–12), 1409–1425. <https://doi.org/10.1016/j.orggeochem.2004.03.008>
- Isobe, K. O., Zakaria, M. P., Chiem, N. H., Le Minh, Y., Prudente, M., Boonyatumanond, R., Saha, M., Sarkar, S., & Takada, H. (2004). Distribution of linear alkylbenzenes (LABs) in riverine and coastal environments in South and Southeast Asia. *Water Research*, 38(9), 2448–2458. <https://doi.org/10.1016/j.watres.2004.02.009>
- Jagoda, A., Żukowski, W., & Dąbrowska, B. (2015). Investigations of the presence of caffeine in the Rudawa River, Kraków. *Poland. Environmental Monitoring and Assessment*, 187(9), 566. <https://doi.org/10.1007/s10661-015-4760-7>
- Kalef, M., Reichert, J., & Demny, G. (2020). Value Engineering als innovativer Lösungsansatz am Beispiel der Kläranlage Düren. *Wiener Mitteilungen*, 252, 35–50.
- Kanzari, F., Syakti, A. D., Asia, L., Malleret, L., Piram, A., Mille, G., & Doumenq, P. (2014). Distributions and sources of persistent organic pollutants (aliphatic hydrocarbons, PAHs, PCBs and pesticides) in surface sediments of an industrialized urban river (Huveaune), France. *Science of the Total Environment*, 478, 141–151. <https://doi.org/10.1016/j.scitotenv.2014.01.065>
- Kasprzyk-Hordern, B., Dinsdale, R. M., & Guwy, A. J. (2008). The occurrence of pharmaceuticals, personal care products, endocrine disruptors and illicit drugs in surface water in South Wales. *UK. Water Research*, 42(13), 3498–3518. <https://doi.org/10.1016/j.watres.2008.04.026>
- Keshavarzifard, M., Zakaria, M. P., Hwai, T. S., Yusuff, F. F. M., Mustafa, S., Vaezzadeh, V., Magam, S. M., Masood, N., Alkhadher, S. A. A., & Abootalebi-Jahromi, F. (2014). Baseline distributions and sources of polycyclic aromatic hydrocarbons (PAHs) in the surface sediments from the Prai and Malacca Rivers. *Peninsular Malaysia. Marine Pollution Bulletin*, 88(1–2), 366–372. <https://doi.org/10.1016/j.marpolbul.2014.08.014>
- Kosma, C. I., Lambropoulou, D. A., & Albanis, T. A. (2010). Occurrence and removal of PPCPs in municipal and hospital wastewaters in Greece. *Journal of Hazardous Materials*, 179(1–3), 804–817. <https://doi.org/10.1016/j.jhazmat.2010.03.075>
- Kubo, A., & Kanda, J. (2017). Seasonal variations and sources of sedimentary organic carbon in Tokyo Bay. *Marine Pollution Bulletin*, 114(2), 637–643. <https://doi.org/10.1016/j.marpolbul.2016.10.030>
- La Farré, M., Pérez, S., Kantiani, L., & Barceló, D. (2008). Fate and toxicity of emerging pollutants, their metabolites and transformation products in the aquatic environment. *Trends in Analytical Chemistry*, 27(11), 991–1007. <https://doi.org/10.1016/j.trac.2008.09.010>
- Lam, M. W., Young, C. J., Brain, R. A., Johnson, D. J., Hanson, M. A., Wilson, C. J., Richards, S. M., Solomon, K. R., & Mabury, S. A. (2004). Aquatic persistence of eight pharmaceuticals in a microcosm study. *Environmental Toxicology and Chemistry*, 23(6), 1431–1440. <https://doi.org/10.1897/03-421>
- Lawrence, J. E., Skold, M. E., Hussain, F. A., Silverman, D. R., Resh, V. H., Sedlak, D. L., Luthy, R. G., & McCray, J. E. (2013). Hyporheic zone in urban streams: A review and opportunities for enhancing water quality and improving aquatic habitat by active management. *Environmental Engineering Science*, 30(8), 480–501. <https://doi.org/10.1089/ees.2012.0235>
- Lin, C., Nguyen, K. A., Vu, C. T., Senoro, D., & Villanueva, M. C. (2017). Contamination levels and potential sources of organic pollution in an Asian river. *Water Science & Technology*, 76(9–10), 2434–2444. <https://doi.org/10.2166/wst.2017.419>
- Lindholm-Lehto, P. C., Ahkola, H. S. J., Knuutinen, J. S., & Herve, S. H. (2016). Widespread occurrence and seasonal variation of pharmaceuticals in surface waters and municipal wastewater treatment plants in central Finland. *Environmental Science and Pollution Research*, 23(8), 7985–7997. <https://doi.org/10.1007/s11356-015-5997-y>
- Löffler, D., Römbke, J., Meller, M., & Ternes, T. A. (2005). Environmental fate of pharmaceuticals in water/sediment systems. *Environmental Science & Technology*, 39(14), 5209–5218. <https://doi.org/10.1021/es0484146>
- Lv, J., Zhang, Y., Zhao, X., Zhou, C., Guo, C., Luo, Y., Meng, W., Zou, G., & Xu, J. (2015). Polybrominated diphenyl ethers (PBDEs) and polychlorinated biphenyls (PCBs) in sediments of Liaohe River: Levels, spatial and temporal

- distribution, possible sources, and inventory. *Environmental Science and Pollution Research*, 22(6), 4256–4264. <https://doi.org/10.1007/s11356-014-3666-1>
- Maaß, A.-L., Esser, V., Frings, R. M., Lehmkuhl, F., & Schüttrumpf, H. (2018). A decade of fluvial morphodynamics: Relocation and restoration of the Inde River (North-Rhine Westphalia, Germany). *Environmental Sciences Europe*, 30(1), 40. <https://doi.org/10.1186/s12302-018-0170-0>
- Matamoros, V., & Salvadó, V. (2012). Evaluation of the seasonal performance of a water reclamation pond-constructed wetland system for removing emerging contaminants. *Chemosphere*, 86(2), 111–117. <https://doi.org/10.1016/j.chemosphere.2011.09.020>
- Matamoros, V., Duhec, A., Albaigés, J., & Bayona, J. M. (2009). Photodegradation of carbamazepine, ibuprofen, ketoprofen and 17 α -ethinylestradiol in fresh and seawater. *Water, Air, & Soil Pollution*, 196(1–4), 161–168. <https://doi.org/10.1007/s11270-008-9765-1>
- MKULNV NRW (2015). *Steckbriefe der Planungseinheiten in den nordrhein-westfälischen Anteilen von Rhein, Weser, Ems und Maas*. Bewirtschaftungsplan 2016–2021: Oberflächengewässer und Grundwasser Teileinzugsgebiet Maas/Maas Süd NRW. Düsseldorf.
- Morehead, M. D., Syvitski, J. P., Hutton, E. W., & Peckham, S. D. (2003). Modeling the temporal variability in the flux of sediment from ungauged river basins. *Global and Planetary Change*, 39(1–2), 95–110. [https://doi.org/10.1016/S0921-8181\(03\)00019-5](https://doi.org/10.1016/S0921-8181(03)00019-5)
- Morin-Crini, N., Lichtfouse, E., & Crini, G. (2021). *Emerging Contaminants Vol. 1: Occurrence and Impact (Vol. 65)*. Springer Nature. <https://doi.org/10.1007/978-3-030-69079-3>
- Net, S., El-Osmani, R., Prygiel, E., Rabodonirina, S., Dumoulin, D., & Ouddane, B. (2015). Overview of persistent organic pollution (PAHs, Me-PAHs and PCBs) in freshwater sediments from Northern France. *Journal of Geochemical Exploration*, 148, 181–188. <https://doi.org/10.1016/j.jgexplo.2014.09.008>
- Niemirycz, E., Gozdek, J., & Koszka-Maron, D. (2006). Variability of Organic Carbon in Water and Sediments of the Odra River and Its Tributaries. *Polish Journal of Environmental Studies*, 15(4), 557–563.
- Notebaert, B., Broothaerts, N., & Verstraeten, G. (2018). Evidence of anthropogenic tipping points in fluvial dynamics in Europe. *Global and Planetary Change*, 164, 27–38. <https://doi.org/10.1016/j.gloplacha.2018.02.008>
- Petrovic, M., Sabater, S., Elosegi, A., & Barceló, D. (2016). *Emerging Contaminants in River Ecosystems. Occurrence and Effects Under Multiple Stress Conditions*. The Handbook of Environmental Chemistry, (Vol. 46). Springer Nature. <https://doi.org/10.1007/978-3-319-29376-9>
- Petts, G.E. (1999). *River regulation*. In *Environmental Geology. Encyclopedia of Earth Science*. Springer, Dordrecht. https://doi.org/10.1007/1-4020-4494-1_283
- Quednow, K., & Püttmann, W. (2009). Temporal concentration changes of DEET, TCEP, terbutryn, and nonylphenols in freshwater streams of Hesse, Germany: Possible influence of mandatory regulations and voluntary environmental agreements. *Environmental Science and Pollution Research*, 16(6), 630–640. <https://doi.org/10.1007/s11356-009-0169-6>
- Rhoads, B. L. (Ed.). (2020). *River dynamics: geomorphology to support management*. Cambridge University Press.
- Schmidt, J.C., & Wilcock, P.R. (2008). Metrics for assessing the downstream effects of dams. *Water Resources Research*, 44(4). <https://doi.org/10.1029/2006WR005092>.
- Schneider, S. L., & Lim, H. W. (2019). Review of environmental effects of oxybenzone and other sunscreen active ingredients. *Journal of the American Academy of Dermatology*, 80(1), 266–271. <https://doi.org/10.1016/j.jaad.2018.06.033>
- Schwanen, C. A., & Schwarzbauer, J. (2022). Structural diversity of organic contaminants in a meso-scaled river system. *Water, Air, & Soil Pollution*, 233(2). <https://doi.org/10.1007/s11270-022-05503-1>.
- Schwanen, C. A., Müller, J., Schulte, P., & Schwarzbauer, J. (2023). Distribution, remobilization and accumulation of organic contaminants by flood events in a meso-scaled catchment system. *Environmental Sciences Europe*, 35(1), 1–16. <https://doi.org/10.1186/s12302-023-00717-4>
- Schwarzbauer, J., & Heim, S. (2005). Lipophilic organic contaminants in the Rhine river, Germany. *Water Research*, 39(19), 4735–4748. <https://doi.org/10.1016/j.watres.2005.09.029>
- Schwarzenbach, R. P., Egli, T., Hofstetter, T. B., von Gunten, U., & Wehrli, B. (2010). Global water pollution and human health. *Annual Review of Environment and Resources*, 35(1), 109–136. <https://doi.org/10.1146/annurev-environ-100809-125342>
- Silva, S., Ferreira, M., Oliveira, A. S., Magalhães, C., Sousa, M. E., Pinto, M., Sousa Lobo, J. M., & Almeida, I. F. (2019). Evolution of the use of antioxidants in anti-ageing cosmetics. *International Journal of Cosmetic Science*, 41(4), 378–386. <https://doi.org/10.1111/ics.12551>
- Skjævrak, I., Brede, C., Steffensen, I.-L., Mikalsen, A., Alexander, J., Fjeldal, P., & Herikstad, H. (2005). Non-targeted multi-component analytical surveillance of plastic food contact materials: Identification of substances not included in EU positive lists and their risk assessment. *Food Additives and Contaminants*, 22(10), 1012–1022. <https://doi.org/10.1080/02652030500090877>
- Staatliches Umweltamt Aachen. (2005). *Ergebnisbericht Rur und südliche sonstige Maaszuflüsse*. Bearbeitungsgebiet Maas-Deutschland (Süd): Wasserrahmenrichtlinie in NRW, Bestandsaufnahme. Düsseldorf.
- Štěpek, J., & Daoust, H. (1983). Plasticizers. In J. Štěpek & H. Daoust (Eds.), *Additives for Plastics* (pp. 7–33). Springer.
- Sternbeck, J., Österås, A. H., & Woldegiorgis, A. (2012). *Screening of TPPO, TMDD and TCEP, three polar pollutants*. Stockholm.
- Sui, Q., Huang, J., Deng, S., Chen, W., & Yu, G. (2011). Seasonal variation in the occurrence and removal of pharmaceuticals and personal care products in different biological wastewater treatment processes. *Environmental Science & Technology*, 45(8), 3341–3348. <https://doi.org/10.1021/es200248d>
- Terasaki, M., Shiraiishi, F., Fukazawa, H., & Makino, M. (2009). Development and validation of chemical and biological analyses to determine the antiestrogenic potency of resin acids in paper mill effluents. *Environmental Science*

- & *Technology*, 43(24), 9300–9305. <https://doi.org/10.1021/es9025479>
- Tockner, K., Uehlinger, U., & Robinson, C. T. (Eds.). (2009). *Rivers of Europe*. Academic Press.
- Vercruyse, K., Grabowski, R. C., & Rickson, R. J. (2017). Suspended sediment transport dynamics in rivers: Multi-scale drivers of temporal variation. *Earth-Science Reviews*, 166, 38–52. <https://doi.org/10.1016/j.earscirev.2016.12.016>
- Vörösmarty, C. J., Meybeck, M., Fekete, B., Sharma, K., Green, P., & Syvitski, J. P. (2003). Anthropogenic sediment retention: Major global impact from registered river impoundments. *Global and Planetary Change*, 39(1–2), 169–190. [https://doi.org/10.1016/S0921-8181\(03\)00023-7](https://doi.org/10.1016/S0921-8181(03)00023-7)
- Wang, J.-Z., Chen, T.-H., Zhu, C.-Z., & Peng, S.-C. (2014). Trace organic pollutants in sediments from Huaihe River, China: Evaluation of sources and ecological risk. *Journal of Hydrology*, 512, 463–469. <https://doi.org/10.1016/j.jhydrol.2014.03.012>
- Wartman, C. A., Hogan, N. S., Hewitt, L. M., McMaster, M. E., Landman, M. J., Taylor, S., Kovacs, T. G., & van den Heuvel, M. R. (2009). Androgenic effects of a Canadian bleached kraft pulp and paper effluent as assessed using threespine stickleback (*Gasterosteus aculeatus*). *Aquatic Toxicology*, 92(3), 131–139. <https://doi.org/10.1016/j.aquatox.2009.02.003>
- Wasserverband Eifel-Rur (2017a). *Die Rurtalsperre*. Düren. Retrieved December 4, 2023, from <https://wver.de/wp-content/uploads/2019/11/Rurtalsperre.pdf>
- Wasserverband Eifel-Rur (2017b). *Die Stauanlage Obermaubach*. Düren. Retrieved December 4, 2023, from https://www.wver.de/wp-content/uploads/2019/11/stb_obermaubach.pdf
- Wasserverband Eifel-Rur (2017c). *Jahresbericht 2016*. Düren. Retrieved December 4, 2023, from <https://wver.de/wp-content/uploads/2019/11/jahresbericht2016.pdf>
- Wasserverband Eifel-Rur (2017d). *Regelungen für die Nutzung des Hauptsees der Rurtalsperre Schwammenauel*. Düren. Retrieved December 4, 2023, from https://wver.de/wp-content/uploads/2019/11/Regelungen_des_WVER_13_10_2017Rurtalsperre_Hauptsee.pdf
- Weatherill, J. J., Atashgahi, S., Schneidewind, U., Krause, S., Ullah, S., Cassidy, N., & Rivett, M. O. (2018). Natural attenuation of chlorinated ethenes in hyporheic zones: A review of key biogeochemical processes and in-situ transformation potential. *Water Research*, 128, 362–382. <https://doi.org/10.1016/j.watres.2017.10.059>
- Westrich, B., & Förstner, U. (2007). *Sediment dynamics and pollutant mobility in rivers: an interdisciplinary approach*. Springer Science & Business Media.
- Wilkinson, J., Hooda, P. S., Barker, J., Barton, S., & Swinden, J. (2017). Occurrence, fate and transformation of emerging contaminants in water: An overarching review of the field. *Environmental Pollution*, 231(1), 954–970. <https://doi.org/10.1016/j.envpol.2017.08.032>
- Wolf, S., Esser, V., Lehmkühl, F., & Schüttrumpf, H. (2022). Long-time impact of a large dam on its downstream river's morphology: Determined by sediment characteristics, pollutants as a marker, and numerical modelling. *Journal of Sedimentary Environments*, 7(3), 403–424. <https://doi.org/10.1007/s43217-022-00103-9>
- Zhang, H., Zhao, X., Ni, Y., Lu, X., Chen, J., Su, F., Zhao, L., Zhang, N., & Zhang, X. (2010). PCDD/Fs and PCBs in sediments of the Liaohe River, China: Levels, distribution, and possible sources. *Chemosphere*, 79(7), 754–762. <https://doi.org/10.1016/j.chemosphere.2010.02.039>
- Zheng, B., Wang, L., Lei, K., & Nan, B. (2016). Distribution and ecological risk assessment of polycyclic aromatic hydrocarbons in water, suspended particulate matter and sediment from Daliao River estuary and the adjacent area, China. *Chemosphere*, 149, 91–100. <https://doi.org/10.1016/j.chemosphere.2016.01.039>

Publisher's Note Springer Nature remains neutral with regard to jurisdictional claims in published maps and institutional affiliations.